Journal of
Technological
Engineering

Journal of Technological Engineering

Definition of Journal

Scientific Objectives

Support the international scientific community in its written production Science, Technology and Innovation in the Field of Engineering and Technology, in Subdisciplines of electromagnetism, electrical distribution, sources innovation in electrical, engineering signal, amplification electrical, motor design science, materials in electrical power, plants management and distribution of electrical energies.

ECORFAN-Mexico SC is a Scientific and Technological Company in contribution to the Human Resource training focused on the continuity in the critical analysis of International Research and is attached to CONACYT-RENIECYT number 1702902, its commitment is to disseminate research and contributions of the International Scientific Community, academic institutions, agencies and entities of the public and private sectors and contribute to the linking of researchers who carry out scientific activities, technological developments and training of specialized human resources with governments, companies and social organizations.

Encourage the interlocution of the International Scientific Community with other Study Centers in Mexico and abroad and promote a wide incorporation of academics, specialists and researchers to the publication in Science Structures of Autonomous Universities - State Public Universities - Federal IES - Polytechnic Universities - Technological Universities - Federal Technological Institutes - Normal Schools - Decentralized Technological Institutes - Intercultural Universities - S & T Councils - CONACYT Research Centers.

Scope, Coverage and Audience

Journal of Technological Engineering is a Journal edited by ECORFAN-Mexico S.C in its Holding with repository in Taiwan, is a scientific publication arbitrated and indexed with semester periods. It supports a wide range of contents that are evaluated by academic peers by the Double-Blind method, around subjects related to the theory and practice of electromagnetism, electrical distribution, sources innovation in electrical, engineering signal, amplification electrical, motor design science, materials in electrical power, plants management and distribution of electrical energies with diverse approaches and perspectives, that contribute to the diffusion of the development of Science Technology and Innovation that allow the arguments related to the decision making and influence in the formulation of international policies in the Field of Engineering and Technology. The editorial horizon of ECORFAN-Mexico® extends beyond the academy and integrates other segments of research and analysis outside the scope, as long as they meet the requirements of rigorous argumentative and scientific, as well as addressing issues of general and current interest of the International Scientific Society.

Arbitration Committee

Assignment of Rights

The sending of an Article to Journal of Systematic Innovation emanates the commitment of the author not to submit it simultaneously to the consideration of other series publications for it must complement the Originality Format for its Article.

The authors sign the Authorization Format for their Article to be disseminated by means that ECORFAN-Mexico, S.C. In its Holding Taiwan considers pertinent for disclosure and diffusion of its Article its Rights of Work.

Declaration of Authorship

Indicate the Name of Author and Coauthors at most in the participation of the Article and indicate in extensive the Institutional Affiliation indicating the Department.

Identify the Name of Author and Coauthors at most with the CVU Scholarship Number-PNPC or SNI-CONACYT- Indicating the Researcher Level and their Google Scholar Profile to verify their Citation Level and H index.

Identify the Name of Author and Coauthors at most in the Science and Technology Profiles widely accepted by the International Scientific Community ORC ID - Researcher ID Thomson - arXiv Author ID - PubMed Author ID - Open ID respectively.

Indicate the contact for correspondence to the Author (Mail and Telephone) and indicate the Researcher who contributes as the first Author of the Article.

Plagiarism Detection

All Articles will be tested by plagiarism software PLAGSCAN if a plagiarism level is detected Positive will not be sent to arbitration and will be rescinded of the reception of the Article notifying the Authors responsible, claiming that academic plagiarism is criminalized in the Penal Code.

Arbitration Process

All Articles will be evaluated by academic peers by the Double Blind method, the Arbitration Approval is a requirement for the Editorial Board to make a final decision that will be final in all cases. MARVID® is a derivative brand of ECORFAN® specialized in providing the expert evaluators all of them with Doctorate degree and distinction of International Researchers in the respective Councils of Science and Technology the counterpart of CONACYT for the chapters of America-Europe-Asia- Africa and Oceania. The identification of the authorship should only appear on a first removable page, in order to ensure that the Arbitration process is anonymous and covers the following stages: Identification of the Journal with its author occupation rate - Identification of Authors and Coauthors - Detection of plagiarism PLAGSCAN - Review of Formats of Authorization and Originality-Allocation to the Editorial Board-Allocation of the pair of Expert Arbitrators-Notification of Arbitration -Declaration of observations to the Author-Verification of Article Modified for Editing-Publication.

Instructions for Scientific, Technological and Innovation Publication

Knowledge Area

The works must be unpublished and refer to topics of Electromagnetism, Electrical distribution, Sources innovation in electrical, Engineering signal, Amplification electrical, Motor design science, Materials in electrical power, Plants management and distribution of electrical energies and other topics related to Engineering and Technology.

Presentation of the content

In the first article we present, *Inductor Disc CFD Analysis for VAWT*, by MARIN-TELLEZ, Gerardo Javier, LÓPEZ-GARZA, Víctor, MARIN-TELLEZ, Paulina and SANTIBAÑEZ-MALDONADO, Adrián, with adscription in the, Universidad Michoacana de San Nicolás de Hidalgo, in the next article we present, *CO_2 emissions of an asphalt pavement in kg of CO_2 per m^2*, by LOPEZ-CHAVEZ, Oscar, MERCADO-IBARRA, Santa Magdalena, ACEVES-GUTIÉRREZ, Humberto and CAMPOY-SALGUERO, José Manuel, with adscription in the, Instituto Tecnológico de Sonora, in the next article we present, *Design and Construction of an ALD Reactor by Growth of Al_2O_3 Nanostructure Films*, by MONTES-GUTIERREZ, Jorge, LOPEZ-GASTELUM, Ana, ROMO-GARCÍA, Frank and GARCIA-GUTIERREZ, Rafael, with adscription in the, Universidad de Sonora, in the next article we present, *Interactive assistant tool for the evaluation of kinematic patterns and EMG signals in patients with a forearm injury*, by JIMÉNEZ-GONZÁLEZ, Fernando C. & TORRES-RAMÍREZ, Dulce Esperanza, with adscription in the, Universidad Tecnológica de Ciudad Juárez.

Content

Article	Page

Inductor Disc CFD Analysis for VAWT

Análisis CFD de Discos Inductores para Turbina Eólica de Eje Vertical

MARIN-TELLEZ, Gerardo Javier†*, LÓPEZ-GARZA, Víctor, MARIN-TELLEZ, Paulina and SANTIBAÑEZ-MALDONADO, Adrián

Universidad Michoacana de San Nicolás de Hidalgo, Mechanical Engineering Faculty

ID 1st Author: *Gerardo Javier, Marin-Tellez* / **ORC ID**: 0000-0002-2613-0570, **CVU CONACYT ID**: 1051543

ID 1st Co-author: *Víctor, López-Garza* / **ORC ID**: 0000-0001-9090-9119, **Researcher ID Thomson**: H-6969-2018, Open ID: 107470673007841597382, **CVU CONACYT ID**: 554311

ID 2nd Co-autor: *Paulina, Marin-Tellez* / **ORC ID**: 0000-0003-2966-3409 **Researcher ID Thomson** G-2113-2019, **CVU CONACYT ID**: 928539

ID 3rd Co-autor: *Adrián, Santibañez-Maldonado* / **ORC ID**: 0000-0003-2090-9556, **CVU CONACYT ID**: 1009460

Abstract

This work shows the computational simulation of the fluid dynamics of inductor discs (patent pending reception number MX/E/2021/002395) applied to vertical axis wind turbines (VAWT). These inductor discs have a unique and innovative design that can be classified as wind concentrators. The purpose of these devices is to increase wind velocity at the wind turbine entrance; this increase in velocity exponentially boosts the mechanical power of the turbine, according to Betz's theory, increasing the electrical energy production of the turbine and, at the same time, reducing its dimensions. The objective of this investigation is to carry out the fluid dynamic simulation (CFD) of two of the inductor disc geometries: an elliptical one and a truncated conical one, varying the entrance wind velocities of the VAWT from 3 m/s to 12 m/s. The proposed methodology consists of employing a CFD software (ANSYS) to model the two inductor disc geometries and extract them from a static control volume. Mesh this volume, establish boundary conditions, and vary wind velocities to carry out the fluid dynamic analysis. Finally, the obtained velocities are compared at different representative points of both geometries.

Resumen

En el presente trabajo, se muestra la simulación computacional de dinámica de fluidos de unos discos inductores (patente en trámite folio de recepción MX/E/2021/002395) con aplicación en turbinas eólicas de eje vertical. Los discos inductores tienen un diseño único e innovador y se pueden clasificar en la categoría de concentradores de eólicos. La finalidad de estos dispositivos es aumentar la velocidad del viento en la entrada de la turbina eólica; con el aumento de esta velocidad la potencia mecánica de la turbina se incrementa exponencialmente de acuerdo con la teoría de Betz, aumentando así la producción de energía eléctrica de la turbina y al mismo tiempo se reducen las dimensiones la misma. El objetivo de esta investigación es realizar la simulación fluidodinámica computacional (CFD) de dos geometrías de discos inductores; una elíptica y otra de cono truncado, variando la velocidad de entrada del viento a la turbina eólica vertical, desde 3 m/s hasta 12 m/s. La metodología propuesta consistió en emplear un software CFD (ANSYS) para modelar las dos geometrías de los discos de inducción y extraerlas de un volumen estático de control. Mallar este volumen, establecer las condiciones de frontera y variar las velocidades del viento para realizar el análisis de dinámica de fluidos. Finalmente se comparan las velocidades obtenidas en diferentes puntos representativos de ambas geometrías.

Simulation, VAWT, Optimization

Simulación, Turbina eólica de eje vertical, Optimización

---

* Correspondence to Author (e-mail: 1422986a@umich.mx)
† Researcher contributing as first author.

1.   Introduction

Renewable energy is the present and future of worldwide electrical energy production. The wind-energy industry is one of the fastest-growing renewable energy technologies and has positioned itself as the second largest renewable energy source of electrical power generation in the world (GWEC, 2019; Subsecretaría de Energía Eléctrica, 2019). Wind turbines can be classified by the orientation of their rotational axes as horizontal axis wind turbines (HAWT) and vertical axis wind turbines (VAWT). A vertical axis wind turbine is a wind machine whose rotational axis is perpendicular to the wind's direction (Presses Internationales Polytechnique, 2002; Yusof & Mohamed, 2020).

Vertical axis wind turbines have several advantages when compared to horizontal axis wind turbines, such as: they are better suited for turbulent winds, changing wind directions, and low-velocity winds. In addition, they have no need of an orientation system, are less noisy, and have a simpler and more compact design (Presses Internationales Polytechnique, 2002; Yusof & Mohamed, 2020).

Vertical axis wind turbines have efficiencies of between 40-50%; this percentage is below the theoretical efficiency of a wind turbine. Therefore, there exists additional potential in bettering this type of turbine so as to increase its efficiency (Yusof & Mohamed, 2020). To better utilize the wind resource in wind turbines, devices called wind concentrators are used. These devices increase the velocity of wind flow at the turbine rotor entrance by employing a specific geometrical configuration that guides the flow upstream or downstream of the device. The purpose of wind concentrators is to achieve a drastic reduction in rotor size while maintaining a low manufacturing cost (García & García, 2012; Hau, 2005).

This present work shows the CFD simulation of inductor discs applied to vertical axis wind turbines. The inductor discs can be classified as wind concentrators, as their objective is to homogenize wind current lines that affect the turbine to increase wind velocity and therefore, achieve a greater energy production in the turbine by means of a passive mechanical device. It must be emphasized that the inductor discs have a unique and innovative design.

This work has as its objective to evaluate and compare two inductor disc geometries, one elliptical, and the other truncated cone, applied to a low-capacity wind turbine using ANSYS software CFX module.

The first section of the article gives a brief introduction to the historical development of vertical axis wind turbines and mentions the most common wind concentrators, as well as the concept of wind turbine potency, to provide the reader with context.

Afterwards, the employed methodology is shown in a general manner, and the next section carries out the dynamic fluid simulation done by ANSYS software CFX module.

The computational fluid dynamics simulations show the two inductor disc geometries which were analyzed, elliptical and truncated cone, as well as the used control volume; they show the mesh in detail, describe the boundary conditions, and present the analyzed wind velocities. Finally, the wind velocity results for each geometry are shown.

2.   Wind Turbines

2.1   Historical Development of Vertical Axis Wind Turbines

The first known practical windmills were built in Sistan in the seventh century and were the first vertical axis windmills. However, it was not until the Cold War and the energetic crisis of 1970 that wind turbines were presented as a competitive source for electrical power generation (Subsecretaría de Energía Eléctrica, 2019; Yusof & Mohamed, 2020).

In 1922, Finnish architect Sigurd Johannes Savonius invented the Savonius turbine; this is the simplest vertical axis wind turbine that exists and is characterized, principally, by its S-shaped blade. The Savonius turbine is a drag device and tends to produce a high starter pair; therefore, it reduces shear velocity and requires a low-velocity wind to start rotating; in addition, it has a lower efficiency than other turbines. It should be noted that conventional Savonius turbines are not suited for electrical power generation due to their inability to rotate faster than the wind (Hau, 2005; Yusof & Mohamed, 2020).

In 1925, French engineer Georges Jean Marie Darrieus invented the Darrieus turbine; this turbine had curved blades that were positioned around a rotating vertical axis. The Darrieus-type turbine showed greater potential than the Savonius, and thus was the center of technological development (Hau, 2005; Yusof & Mohamed, 2020).

Two principal configurations for the Darrieus turbine were developed: straight blades and curved blades. The curved-bladed configuration evolved from a conventional cable-fastening base to a fixed tower base, and finally, to a vertical cantilevered base (Hau, 2005; Yusof & Mohamed, 2020).

Meanwhile, straight-bladed configurations underwent multiple variations: a changeable geometry, the Musgrove rotor; a changeable pace, the Giromill rotor; a changeable diamond-rotor configuration, Delta, in either V-shape or Y-shape. However, they did not prosper, due to the high specific cost of energy (Hau, 2005; Yusof & Mohamed, 2020).

The Musgrove rotor survived and evolved into a configuration in which the blades formed an H-shape, with straight blades and fixed pace, simply named H rotor. The H rotor also underwent variations: articulated, inclined, and helicoidal H rotors. There have also been a few hybrid designs using Savonius and Darrieus rotors (Hau, 2005; Yusof & Mohamed, 2020).

2.2 Wind-Energy Concentrators

The basic idea of a wind-energy concentrator is to increase potential performance in relation to rotor sweep area by employing a static structure (Hau, 2005).

This idea can be traced back to the first days of windmill history, as shown by ancient windmill drawings from the Middle East. The most studied and known wind concentrators are as follows (Hau, 2005; Shonhiwa & Makaka, 2016):

Conducted rotor: this is the simplest method and consists of confining the rotor in a duct. The potential coefficient that can be obtained by this method is 0.66 (Hau, 2005; Shonhiwa & Makaka, 2016).

Diffuser-duct turbine: as its name indicates, a funnel-shaped duct is placed behind the rotor, creating a diffuser. It can reach a potential coefficient of 0.75 (Hau, 2005).

Vortex tower: in a tower with adjustable slots placed in the cylinder liner, the wind flows tangentially towards the interior of the duct, where an air vortex, like a tornado, is formed. Due to the low pressure at the center of the vortex, the air is sucked from the bottom part of the tower into the duct, propelling in that manner a turbine with a diameter of approximately one-third of the tower's diameter (Hau, 2005).

2.2 Wind Turbine Potency

The potency generated by a wind turbine is determined by the following equation:

$$P = \frac{1}{2} C_p A \rho_{aire} V^3 \qquad (1)$$

Where P is the mechanical potency of the turbine, C_p is the potential coefficient specific to the turbine, A is the cross-sectional area of the turbine through which the wind flows, ρ is the air density, and V is the wind velocity before entering the rotor (Presses Internationales Polytechnique, 2002; Shonhiwa & Makaka, 2016).

As shown in equation 1, wind turbine potency depends on 4 factors (C_p, A, ρ_{aire} and V); in each case, it is directly proportional to them; that is, if we increase any of these factors, the potency of the turbine also increases.

C_p is specific to each turbine model; ρ_{air} depends on the site where the turbine will be installed and varies, principally, depending on the elevation and the annual average temperature of the site; in a similar manner, A depends on the shape of the turbine; and V depends on many factors, such as topographical and climatological ones. In general, V is the most important factor, since its value has a cubed implication on the potency; for example, if the wind velocity doubles, the potency increases 800% (Presses Internationales Polytechnique, 2002; Shonhiwa & Makaka, 2016). To emphasize even further the importance of wind velocity, according to Betz's theory, rotor diameters are inversely proportional to wind velocity.

Therefore, rotor diameter sizes and wind turbines significatively decrease when wind velocity increases (Presses Internationales Polytechnique, 2002; Shonhiwa & Makaka, 2016).

3. Methodology

Overall, the followed methodology was to model the two proposed inductor disc geometries (elliptical and truncated cone) using the DesignModeler module in ANSYS Workbench software. The CFX module of ANSYS software was used to analyze the computational fluid dynamics; a control volume was modelled and both geometries were meshed. After meshing, boundary conditions were established, including different wind velocities. Finally, the simulation was run, and the results were analyzed. See Graph 1.
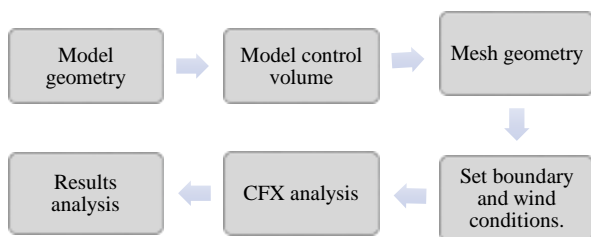
Graph 1 General methodology
Source: Authors' Own Creation

4. Computational Fluid Dynamics Simulation

4.1 Inductor Disc Geometries

The first evaluated induction disc geometry has an elliptical shape; the second geometry has a truncated-cone shape. To compare these geometries, the same diameter was considered, 2.8 times greater than the turbine diameter (wind turbine diameter 2.3 m), and the cross-sectional area where the turbine was placed was also the same in both geometries, shown as a dark gray color in Figure 1. The narrowest section in the shaded area is 1.6 m, slightly taller than the wind turbine blade height (blade height 1.5 m). To compare the performance of the inductor discs, these were designed in such a way that the reduction area occasioned by each of these geometries, corresponding to the cross-sectional area of the inductor discs at the frontal face of the control volume, was the same. This is represented graphically in Figure 1.

A big-enough computational domain was employed, to prevent the walls from being too close to the discs and affecting the development of wind flow. Deducting the cross-sectional disc area from the control volume frontal face area, the percentage of free area through which the wind can circulate is 97.9%, shown as a shaded area in Figure 2.
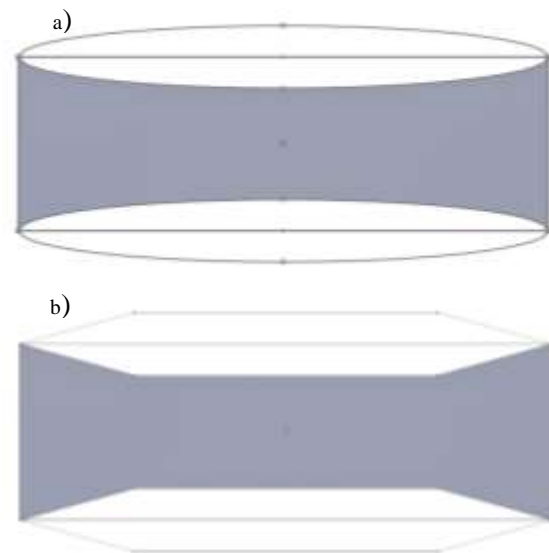
Figure 1 Induction cross-sectional areas of the evaluated geometries. a) Elliptical b) Truncated cone
Source: Authors' Own Creation
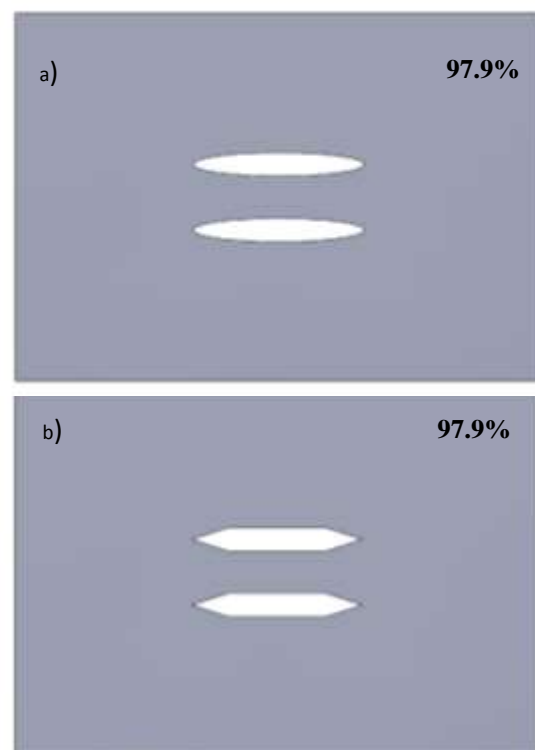
Figure 2 Representation of reduction area percentage. a) Elliptical. b) Truncated cone
Source: Authors' Own Creation

4.2 Control Volume

A static volume was modelled, comprising of a rectangular prism 22 m wide by 20 m high by 30 m long.

During the simulation, the wind flows through the smaller faces of the rectangular prism (Face A and Face B); the inlet face is closest to the wind turbine, Face A, located 10 m from the center of the rotor. The furthest face is the outlet face, Face B, located 20 m from the center of the rotor; the intention of having a greater length downstream is to appreciate the formation of tailwinds after having passed through the discs. See Figure 3.
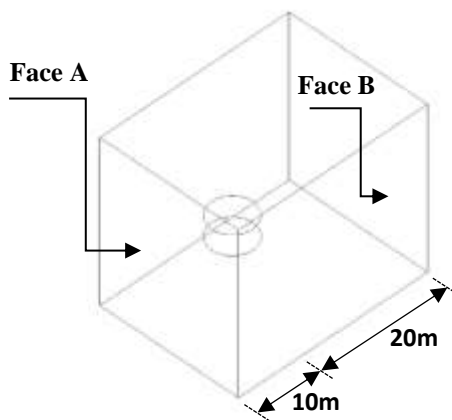
Figure 3 Control volume
Source: ANSYS (Academics)

4.3 Mesh

A non-structured mesh with tetrahedral and triangular-prism elements was used in both geometries. The tetrahedral elements predominate, and the triangular-prism elements were inflated around the zone of the inductor discs as shown in Figures 4-7.

A mesh refinement was used in both geometries around the induction discs, using the influence sphere method; the center of the sphere corresponds to the center of the induction discs in the middle of the height that separates them.

The elliptical geometry mesh has approximately 3.7 million elements, while the truncated-cone geometry mesh has approximately 3.6 million elements.
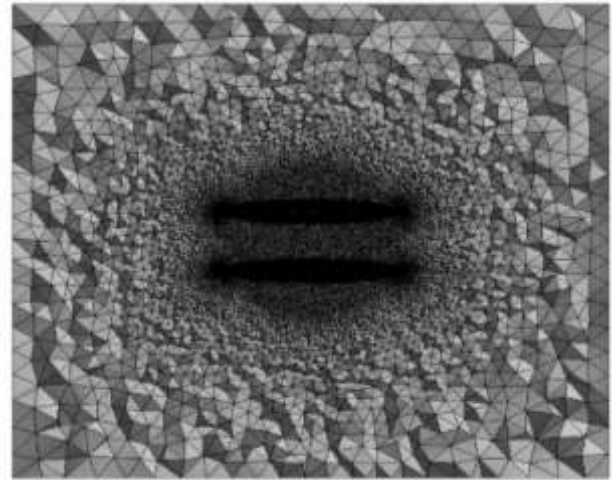
Figure 4 Cross section of elliptical geometry mesh
Source: ANSYS (Academics)
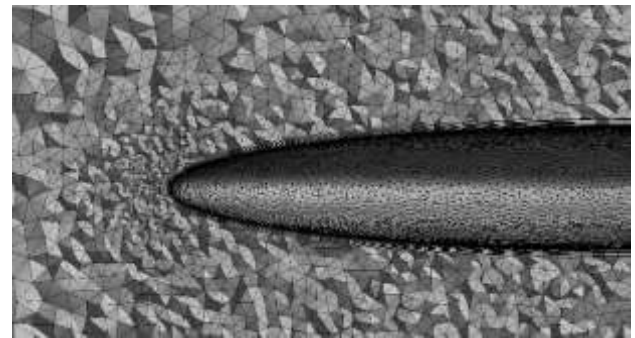
Figure 5 Refinement detail in induction disc zone of elliptical geometry. *Source: ANSYS (Academics)*

Figure 6 Cross section of truncated-cone geometry mesh. *Source: ANSYS (Academics)*
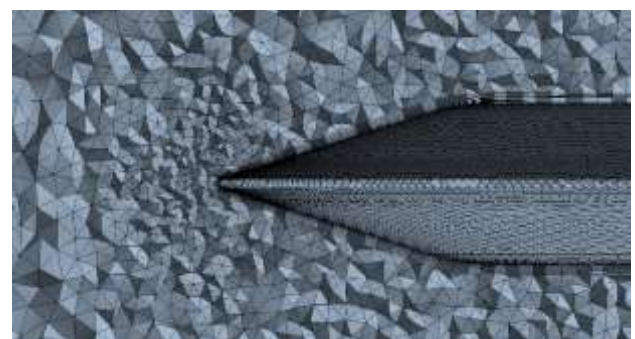
Figure 7 Refinement detail in induction disc zone of truncated-cone geometry. *Source: ANSYS (Academics).*

MARIN-TELLEZ, Gerardo Javier, LÓPEZ-GARZA, Víctor, MARIN-TELLEZ, Paulina and SANTIBAÑEZ-MALDONADO, Adrián. Inductor Disc CFD Analysis for VAWT. Journal of Technological Engineering. 2021

4.4   Boundary conditions

Face A was defined as the inlet of a constant-velocity and uniform wind; Face B, as the outlet of wind flow at atmospheric pressure; and the wind velocities at the adjacent faces were identical in magnitude and direction to the inlet velocity.

Wind velocity varied in a range from 3 to 12 m/s. Standard air conditions for temperature, density, and dynamic viscosity were considered.

5.   Results

The obtained data from the simulation are the increases in wind velocity due to the induction discs. Twenty-one representative points were sampled across three planes; in other words, seven points per plane: Frontal Disc (DF), Posterior Disc (DP), Frontal Rotor (RF), Posterior Rotor (RP), Left Rotor (RI), Right Rotor (RD), and Center (C).

The central plane is in the middle of the distance between the inductor discs; the top plane is in the space that separates the induction disc and the top part of the wind turbine rotor: the bottom plane is in the space that separates the induction disc and the bottom part of the wind turbine rotor. See Figures 8 and 9.
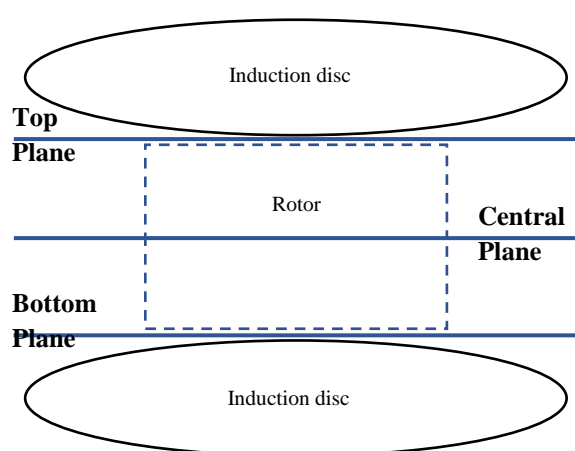
**Figure 8** Cross-sectional view of used reference planes
Source: Authors' Own Creation
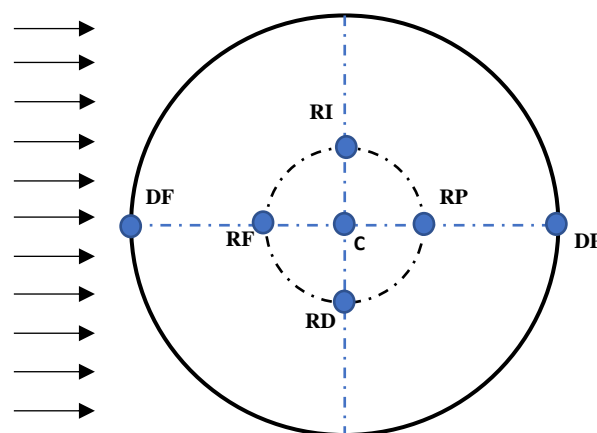
Figure 9 Top view of used reference planes
Source: Authors' own creation

In Figures 10 and 11, the velocity contours for the induction discs with elliptical geometry are shown, at an inlet velocity of 12 m/s.

In Figures 12 and 13, the velocity contours for the induction discs with truncated-cone geometry are shown, at an inlet velocity of 12 m/s.

It can be observed that, in fact, the wind accelerates in a much more homogeneous manner with elliptical inductor discs, since with truncated-cone ones, there are concentration zones.
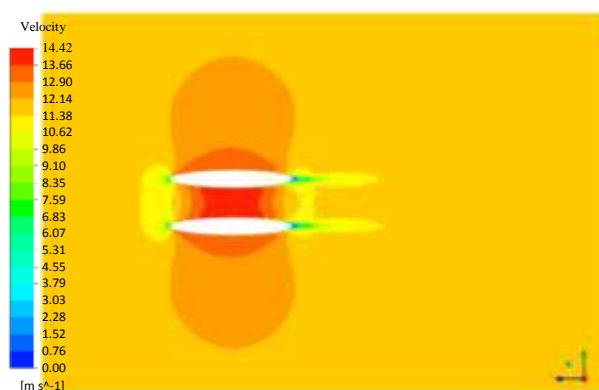
Figure 10 Wind velocity contours perpendicular to lateral face of elliptical geometry. Inlet wind velocity 12 m/s
Source: ANSYS (Academics)
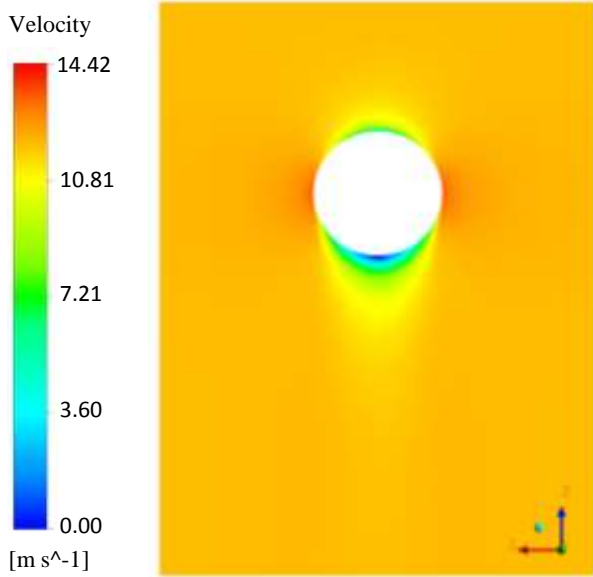
Figure 11 Wind velocity contours perpendicular to top face of elliptical geometry. Inlet wind velocity 12 m/s
Source: ANSYS (Academics)
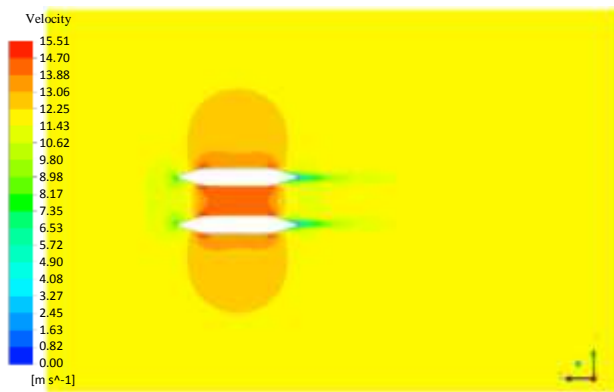
Figure 12 Wind velocity contours perpendicular to lateral face of truncated cone geometry. Inlet wind velocity 12 m/s. *Source: ANSYS (Academics)*
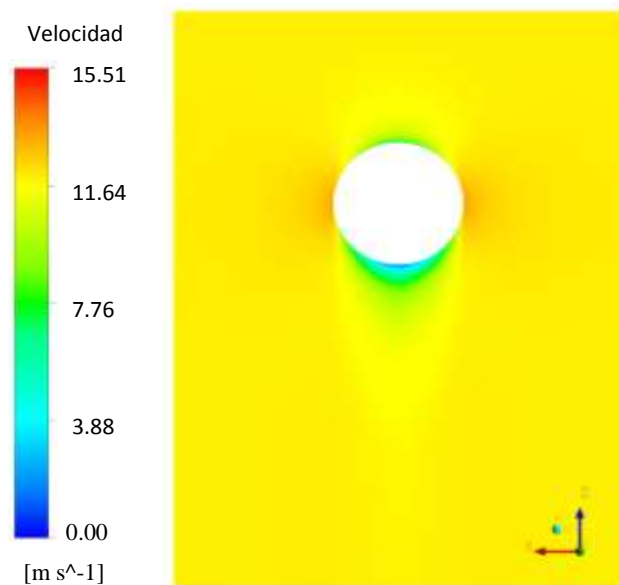
Figure 13 Wind velocity contours perpendicular to top face of truncated cone geometry. Inlet wind velocity 12 m/s
Source: ANSYS (Academics)

In Graphs 2-10, the results for the discs with truncated-cone geometry are shown in orange, and the results for the discs with elliptical geometry are shown in blue.

In Graphs 2-5, the data for wind velocity at each of the seven points in each plane for inlet velocities of 3, 6, 9, and 12 m/s are shown. The first five points, which are DF, RF, C, RP, and DP, are ordered in such a way that allows for the following of the changes in wind velocity, since these points are located along the plane that is perpendicular to the wind face; see Figure 10 and Figure 12. The last two points pertain to where the rotor blades would be located; see Figure 9. The bars in Graphs 2-5 are ordered so that, along the central plane, the data for the elliptical discs are shown, and then, along the same plane, the data for the truncated-cone discs.

Based on Graphs 2-5, it can be observed that the wind velocity tendencies are practically identical in both top and bottom planes at their respective points (DF, DP, RF, RP, RI, RD, and C). This is to be expected due to the geometrical symmetry of the discs in relation to the central plane and the constant and uniform inlet velocity. It can also be observed that the velocity varies in greater measure along the central plane.

In the same manner, Graphs 2-5 are representative of the model, since the pattern shown is preserved for the missing velocities of 4, 5, 7, 8, 10, and 11 m/s.
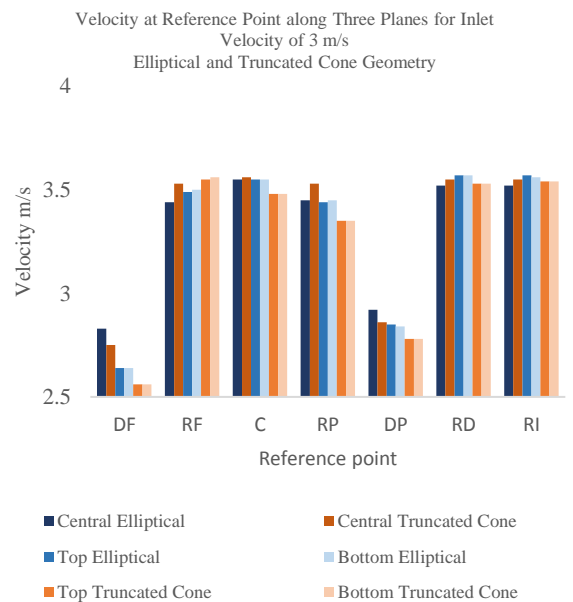
Graph 2 Velocity at each reference point along the three planes for an inlet velocity of 3 m/s, elliptical and truncated cone geometries
Source: Authors' Own Creation

MARIN-TELLEZ, Gerardo Javier, LÓPEZ-GARZA, Víctor, MARIN-TELLEZ, Paulina and SANTIBAÑEZ-MALDONADO, Adrián. Inductor Disc CFD Analysis for VAWT. Journal of Technological Engineering. 2021
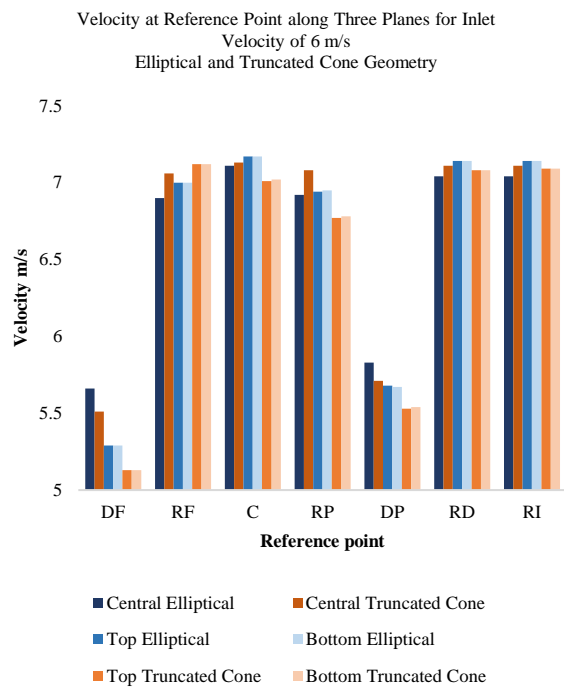
Graph 3 Velocity at each reference point along the three planes for an inlet velocity of 6 m/s, elliptical and truncated cone geometries
Source: Authors' Own Creation

Graph 5 Velocity at each reference point along the three planes for an inlet velocity of 12 m/s, elliptical and truncated cone geometries
Source: Authors' Own Creation

In Graphs 6-8, the behavior of the velocity as it passes through the discs is analyzed in greater detail (see Figures 10 and 12), comparing the two geometries along the top (Graph 6), central (Graph 7), and bottom (Graph 8) planes. Graphs 6-8 are characteristic to the model, since the pattern repeats itself for the other velocities; an inlet velocity of 12 m/s was used so that these coincide with the velocity in Figures 10-13.

In Graphs 6-8, it can be observed with greater detail the practically identical behavior between the top and bottom planes due to symmetry.

The elliptical geometry follows the same pattern in wind velocity change along the three planes (top, central, and bottom), increasing up to the central point (C) and subsequently decreasing until exiting the disc (DP). In the truncated-cone geometry, however, a different pattern along the central plane is observed, where there is an abrupt increase between points DF and RF; afterwards, a slighter increase (between RF and RP); and finally, an abrupt decrease between RP and DP; in contrast, along any of the other two planes (top or bottom), this behavior is inverted, as there is an abrupt increase between points DF and RF, but then a slow decrease between RF and RP, and finally, an abrupt decrease between RP and DP.

Graph 4 Velocity at each reference point along the three planes for an inlet velocity of 9 m/s, elliptical and truncated cone geometries
Source: Authors' Own Creation

MARIN-TELLEZ, Gerardo Javier, LÓPEZ-GARZA, Víctor, MARIN-TELLEZ, Paulina and SANTIBAÑEZ-MALDONADO, Adrián. Inductor Disc CFD Analysis for VAWT. Journal of Technological Engineering. 2021

For the most part, it can be observed that the truncated-cone geometry has more abrupt changes in wind velocity compared to the elliptical geometry.

Velocity at Reference Point along Top Plane for
Inlet Velocity of 12 m/s
Elliptical and Truncated Cone Geometry

Graph 6 Velocity at each reference point along the top plane for an inlet velocity of 12 m/s, elliptical and truncated cone geometries
Source: Authors' Own Creation

Velocity at Reference Point along Central Plane for
Inlet Velocity of 12 m/s
Elliptical and Truncated Cone Geometry
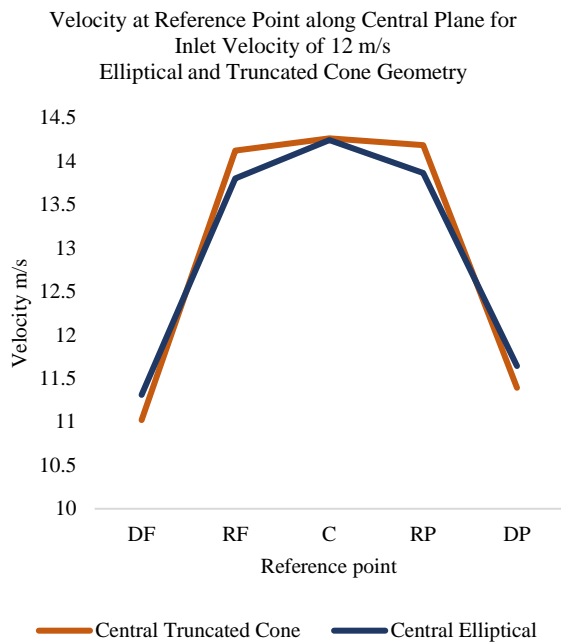
Graph 7 Velocity at each reference point along the central plane for an inlet velocity of 12 m/s, elliptical and truncated cone geometries
Source: Authors' Own Creation

Velocity at Reference Point along Bottom Plane for
Inlet Velocity of 12 m/s
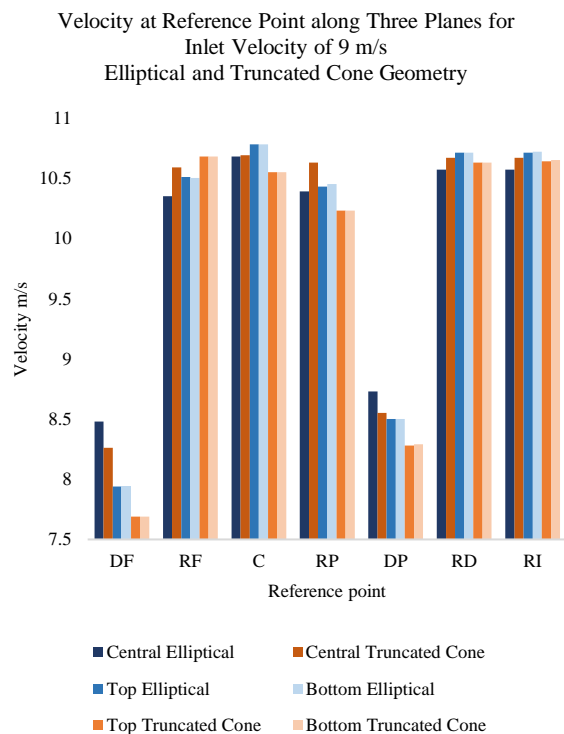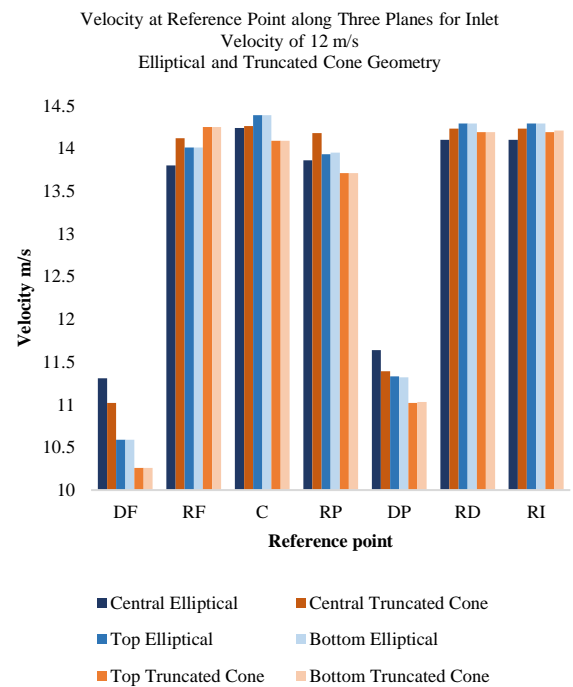Elliptical and Truncated Cone Geometry
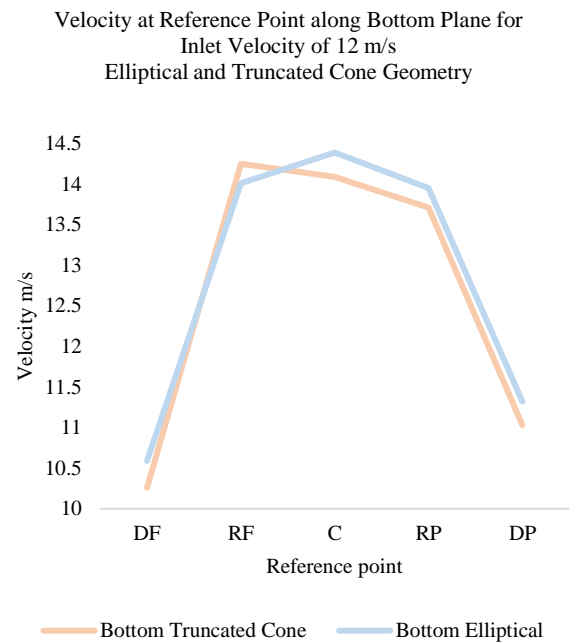
Graph 8 Velocity at each reference point along the bottom plane for an inlet velocity of 12 m/s, elliptical and truncated cone geometries
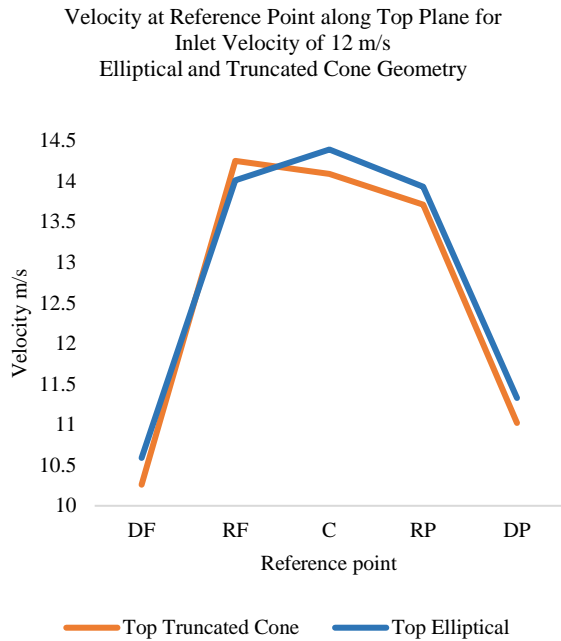*Source: Authors' Own Creation*

In Graphs 9 and 10, the values of the velocity at points RD, C, and RI along the three planes (Graph 9 for top and bottom planes and Graph 10 for central plane) are graphed. Graphs 9-10 are characteristic to the model, since the pattern repeats itself for the other velocities; an inlet velocity of 12 m/s was used so that these coincide with the velocity in Figures 10-13. In Graphs 9-10, the symmetry of results between the values along the top and bottom planes can be observed; in addition, another symmetry of results between the left and right sides is also presented and expected, due to the symmetry of the control volume in relation to the plane perpendicular to the lateral face of the geometry.

In Graph 9, the truncated cone presents greater velocities at the edges than in the center along the top and bottom planes. However, in Graph 10, the velocity at the center is greater than those at the edges along the central plane; nonetheless, the difference is small. The elliptical discs in Graphs 9-10 present the similar behavior of possessing a greater velocity at the center than at the edges. Even though the difference between the velocities at the edges and in the center is larger, the elliptical geometry has the advantage of presenting the same behavior along the three planes, while the truncated-cone geometry inverts its behavior along the central plane when compared to the top and bottom planes.

MARIN-TELLEZ, Gerardo Javier, LÓPEZ-GARZA, Víctor, MARIN-TELLEZ, Paulina and SANTIBAÑEZ-MALDONADO, Adrián. Inductor Disc CFD Analysis for VAWT. Journal of Technological Engineering. 2021

Velocity at Reference Point along Top and Bottom
Planes for Inlet Velocity of 12 m/s
Elliptical and Truncated Cone Geometry

Graph 9 Velocity at each reference point along the top and bottom planes for an inlet velocity of 12 m/s, elliptical and truncated cone geometries
Source: Authors' Own Creation

Velocity at Reference Point along Central Plane for
Inlet Velocity of 12 m/s
Elliptical and Truncated Cone Geometry

Graph 10 Velocity at each reference point along the central plane for an inlet velocity of 12 m/s, elliptical and truncated cone geometries
Source: Authors' Own Creation

6. Acknowledgements

7. Conclusions
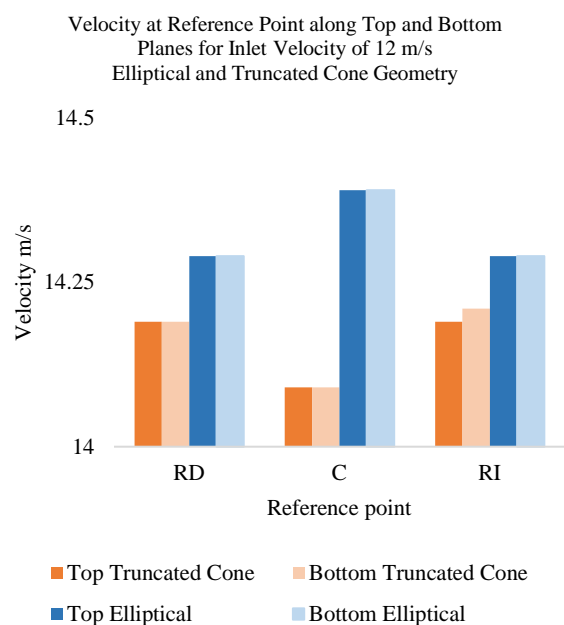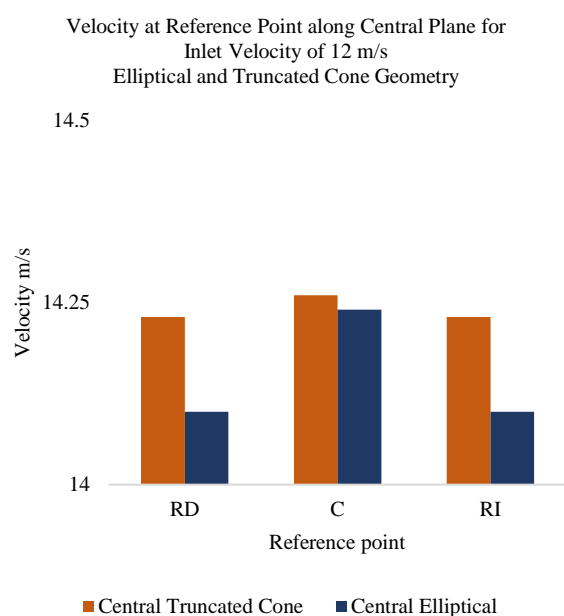
The inductor discs produced a Venturi effect, hence increasing the wind velocity around the rotor area by 15% compared to the inlet wind velocity. This 15% rise could be harnessed by vertical axis wind turbines and increase their power generation by up to 50%.

The inductor discs increase wind velocity by producing a Venturi effect; this increase in wind velocity can be harnessed by vertical axis wind turbines to enhance their performance.

The elliptical inductor discs produced a more homogeneous acceleration than the truncated-cone inductor discs, which in turn could result in lower stress on the wind turbine and a lower turbulence, increasing rotor durability and enhancing its performance.

The truncated cone discs have the advantage of further increasing wind velocity in rotor blade areas, compared to the elliptical discs, although the difference is not considerable. However, the concentration zones around the truncated-cone discs increase the possibility of accentuating or increasing turbulence with an operating rotor.

The elliptical inductor discs offer to be the best option as a concentrator, even though its manufacturing could be more complicated due to its shape, compared to the truncated-cone disc.

References

Burton, T., Sharpe, D., Jenkins, N., & Bossanyi, E. (2001). *Wind Energy Handbook* (Jonh Wiley).

García, E. J., & García, B. (2012). *Tesis doctoral Modelización de un captador eólico de alta eficiencia*.

GWEC. (2019). *GWEC Global Wind Report 2019*. https://gwec.net/wp-content/uploads/2020/08/Annual-Wind-Report_2019_digital_final_2r.pdf

Hau, E. (2005). *Wind Turbines Fundamentals, Technologies, Application, Economics* (Springer (ed.); 2a ed.).

Presses Internationales Polytechnique. (2002). *Wind Turbine Design with Emphasis on Darrieus Concept.*

S. Shikha, T.S.Batí, & D.P.Kpthari. (2003). A new vertical axis wind rotor using convergent nozzles. *Large Enginering Conference on Power Energy*, 177–181.

Shonhiwa, C., & Makaka, G. (2016). Concentrator Augmented Wind Turbines: A review. *Renewable and Sustainable Energy Reviews*, *59*, 1415–1418. https://doi.org/10.1016/j.rser.2016.01.067

Subsecretaría de Energía Eléctrica. (2019). *Energía Eolica.* http://www.energia.gov.ar/contenidos/archivos/ publicaciones/libro_energia_eolica.pdf

Yusof, A., & Mohamed, M. R. (2020). Vertical Axis Wind Turbines: An Overview. *Lecture Notes in Electrical Engineering*, *632*, 821–835. https://doi.org/10.1007/978-981-15-2317-5_68

CO₂ emissions of an asphalt pavement in kg of CO₂ per m²

Emisiones de CO₂ de un pavimento asfáltico en kg de CO₂ por m²

LOPEZ-CHAVEZ, Oscar†, MERCADO-IBARRA, Santa Magdalena, ACEVES-GUTIÉRREZ, Humberto* and CAMPOY-SALGUERO, José Manuel

Instituto Tecnológico de Sonora

ID 1st Author: *Oscar, Lopez-Chavez* / **ORC ID**: 0000-0002-1415-6116

ID 1st Co-author: *Santa Magdalena, Mercado-Ibarra* / **ORC ID**: 0000-0002-4417-0736, **Researcher ID Thomson**: H-3386-2018, **CVU CONACYT ID**: 258533

ID 2nd Co-author: *Humberto, Aceves-Gutiérrez* / **ORC ID**: 0000-0001-9916-3114, **Researcher ID Thomson**: F-8970-2018, **CVU CONACYT ID**: 2811581

ID 3rd Co-author: *José Manuel, Campoy-Salguero* / **ORC ID**: 0000-0002-7110-3256

Abstract

Climate change is one of the world's major problems and concerns the entire human population as its effects are global in scope. Climate change is driven by the greenhouse effect, which is generated by greenhouse gases (GHG). The construction industry is important in the development of a country, both economically and culturally, since it is through it that the infrastructure needs required for a nation's economic and social activities are met. Urban environments are composed of various structures that favor economic, social and any other activities of interest within the existing population; such urban environment is mainly connected by a system that is constituted by asphalt pavements of flexible or rigid type. This project analyzes the environmental impacts generated during the construction process of an asphalt pavement corresponding to the Real de Sevilla III subdivision, located in Obregon City, Sonora, Mexico, applying the Simapro 9.0 Software, obtaining a result of 12.618 Kg CO₂ eq/m2 and 1,140, 863.493 Kg-CO₂/fractionation generated by its main materials and activities and equipment consumptions.

Resumen

El cambio climático es uno de los principales problemas a nivel mundial, concierne a toda la población humana ya que sus efectos son de alcance global. El cambio climático es impulsado por el efecto invernadero, el cual es generado por los gases del mismo nombre (GEI). La industria de la construcción es importante en el desarrollo de un país, en los ámbitos económico y cultural, ya que, a través de ella se satisfacen las necesidades de infraestructura que requieren las actividades económicas y sociales de una nación. Los entornos urbanos se componente de diversas estructuras que favorecen las actividades económicas, sociales y de cualquier otro interés dentro de la población existente, tal entorno urbano está conectado principalmente por un sistema que está constituido por pavimentos asfálticos de tipo flexible o rígido. En el presente proyecto se analiza los impactos ambientales generados durante el proceso de construcción de un pavimento asfáltico correspondiente al fraccionamiento Real de Sevilla III, ubicado en ciudad Obregón Sonora, México, aplicando el Software Simapro 9.0, obteniendo un resultado de 12.618 en kg de CO₂ eq/m2 y de 1, 140,863.493 kg de CO₂ eq. /fraccionamiento generado por sus principales materiales y actividades y consumos de los equipos.

Carbon footprint, CO2, Pavement

Huella de carbono, CO₂, Pavimento

---

* Correspondence to Author (e-mail: haceves_itson@hotmail.com)
† Researcher contributing as first author.

Introduction

Human beings develop their lives in a physical space surrounded by other organisms and the physical and socio-economic environment in which biotic and abiotic factors interact with each other generating a place of their own and this space is called environment (Marino, 2009).

Human beings have always maintained a close relationship with nature from which they have obtained food, fuel and various materials for their survival, including raw materials for the manufacture of clothing, housing and other types of infrastructure, among many other products (Semarnat, 2012).

Until not so long ago, the capacity of humans to alter the environment was limited and punctual. But in the last hundred years, this capacity to alter the environment has increased significantly, to the point of endangering the entire planet (Cidead, 2018). The environment has to some extent withstood human activities with a degree of adequacy, producing desired goods and products, which have caused emissions or discharges to air, water and land (Encinas, 2011).

Air emissions have led to air pollution, which continues to wreak havoc on human health and is estimated to affect 90% of the world's population and is responsible for the premature death of seven million people each year, including 600,000 children (UN, 2019).

Atmospheric emissions, discharges or non-visible waste generated by industries are undoubtedly the most damaging of the waste produced by human activities. Their invisibility, together with the spatial and/or temporal distances at which they can manifest themselves, is one of their worst effects, as it leads to a disregard that is absolutely unacceptable when viewed from the perspective of sustainability requirements (Ripoll & Del Cerro, 2007).

The United Nations (UN) (2019), has pointed out that this type of air pollution is a "silent killer" and highlights that it does not receive due attention "as these deaths are not as tragic as those caused by disasters or epidemics". He also points out that air pollutants are mainly caused by the burning of fossil fuels for electricity production, transport, heating, industrial activity and poor waste management.

These emissions have led to what in recent decades has come to be known as climate change, which according to the Intergovernmental Panel on Climate Change (IPCC) (2014), is the change in the state of the climate, identifiable (through statistical evidence) in changes in the mean value or in the variability of its properties, that persists over long periods of time, usually decades or longer.

Climate change is driven by the greenhouse effect, which is generated by the greenhouse gases of the same name "greenhouse gases" (GHGs). GHGs are a natural part of the planet's climatic conditions, they provide optimal conditions for life on planet earth, ensuring an ideal temperature for natural processes to take place, without them the planet would have lower temperatures which would not allow the development and growth of living things (Florides, Christodoulides, & Messaritis, 2013).

The greenhouse gases that occur naturally in the atmosphere are: water vapour, carbon dioxide (CO_2), nitrous oxide (N_2O), methane (CH_4), and ozone (O_3), which are responsible for absorbing and emitting certain radiation from the earth's surface, atmosphere and clouds. The problem occurs when there is an increase in the concentration of these gases, as the radiation absorbed and emitted by the atmosphere is greater, causing the temperature of the Earth's surface and the troposphere to rise (UNAM, 2018).

According to Figure 1, total anthropogenic GHG emissions have continued to increase between 1990 and 2019, with the largest absolute increases between 2000 and 2019, despite a growing number of climate change mitigation policies.
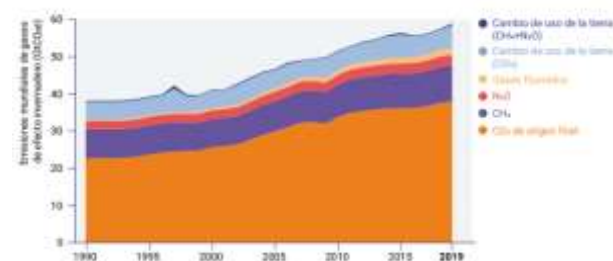
Figure 1 Total annual anthropogenic GHG emissions by gas, 1990-2019
Source: UN, 2020

Among the main GHGs, carbon dioxide (CO_2) is of most concern because of its responsibility for climate change and according to OECC (2014), the concentration of CO_2 in the atmosphere has increased due to human activity, primarily fossil fuel use and deforestation, with a minor contribution from cement production. It is also noted that current concentrations of CO_2, CH_4 and N_2O substantially exceed the range of concentrations recorded in ice cores over the past 800,000 years. The rate of increase in atmospheric concentrations of CO_2, CH_4 and N2O in the past 20th century is unprecedented in the last 22,000 years, as they have increased since 17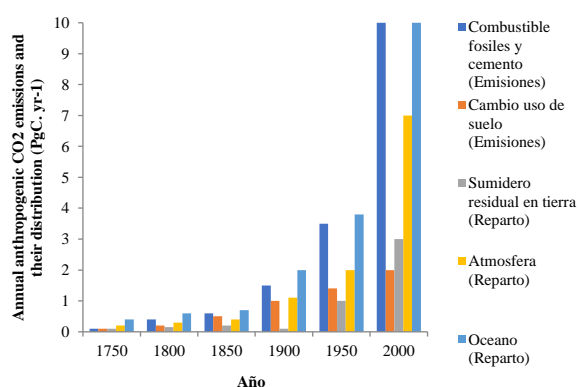50, exceeding pre-industrial levels by 40%, 150% and 20%, respectively, and finally the pH of ocean water has decreased by 0.1 since the beginning of the industrial era, which corresponds to a 26% increase in hydrogen ion concentration (see Figure 2).

Figure 2 Annual anthropogenic CO_2 emissions and their distribution (PgC.year)
Source: OECC, 2014

According to Semarnat (2015), the effects produced by the emission and accumulation of GHGs include extreme changes in environmental temperature, precipitation, winds, an increase in the frequency of extreme weather events such as increased flooding in some regions with decreased rainfall and increased droughts in others, melting of the polar ice caps and continental glaciers. In addition, with the result of severe flooding and rising global sea levels, the migration of flora and fauna from one latitude to another, an increase in diseases, especially infectious and contagious diseases, and finally variations in the cycle and intensity of hurricanes, among many others, most of which have negative effects.

(Soto, González, & Fernández, 2013), state that the increase in carbon concentrations in the atmosphere acidifies the oceans, which affects marine biodiversity. Terrestrial biodiversity is influenced by climate variability, such as extreme weather events (e.g. droughts or floods) that influence the sustainable productivity of soils; hence, adequate nutrition.

The World Health Organisation (WHO) has estimated the number of deaths attributable to climate change at 160,000 per year; however, in 2003 the effects of the heat wave exceeded forecasts, with 70,000 more deaths than expected occurring in Europe that summer (Sunyer, 2010).

In the second half of the 21st century, heat waves are predicted to become more frequent and extreme in parts of Europe and North America. As this pattern becomes more pronounced, extreme heat waves will affect the Mediterranean area, southern and western United States (Soto, et al, 2013).

The environmental impact that industries have on the environment and natural resources has been considerable, not only as a result of the growth in production but also because this growth has been concentrated in sectors with high environmental impact. Among the industrial sectors that most affect the environment are basic petrochemicals, chemicals and metallurgy, which together may account for more than half of the pollution generated by the industrial sector. In terms of hazardous waste, the chemical, metallurgical and automotive industries are the industrial sectors with the highest generation, followed by the electricity and food industries (Semarnat, 2010).

The construction sector uses inputs from other industries such as steel, iron, cement, sand, lime, wood, among others. Construction has numerous negative effects on the environment, among the most notable are: pollution, excessive use of materials with the consequent loss of natural resources, degradation of landscape quality and alteration of natural drainage (Acosta B., 2019).

The soil is altered due to the waste that comes from the dumping of construction waste and debris with numerous negative effects on the environment, among which are pollution, degradation of landscape quality and alteration of natural drainage, this generates the impacts of acidification, eutrophication and eco-toxicity which causes modification generated to the ecosystem (Acosta D., 2002).

In addition, earth movement generates alterations to geomorphology, the loss of vegetation cover causes faster erosion processes and sometimes, when explosives are used for excavations in the construction industry, slope instability can be generated (Arenas, 2010). Disturbances in the air are associated with dust, noise, CO_2 emissions from the use of fossil fuels, minerals, excavation works, cutting of slopes and operation of machines and tools.

(Medineckiene, Kazimieras, & Turskis, 2010), highlight that the use of minerals as construction material generates fine dust particles during its degradation process, according to the dispersion, the most dangerous of them are hard particles of class 5°, which are not stopped by the upper respiratory tract of humans, causing problems in the mucous membrane of the nose, trachea, bronchial tubes, which cause inflammatory reactions and eventually chronic disturbances and then people get respiratory tract diseases, such as bronchitis, tracheitis and pneumonia (diffuse sclerosis of the lungs).

The commercial and residential construction sector generates 39% of the CO_2 emitted into the atmosphere, as well as 30% of the solid waste and 20% of the water pollution. It is therefore concluded that half of the CO_2 emitted into the atmosphere is related to the construction of buildings and construction sites of all types throughout all phases: construction, use and subsequent demolition (Growing Buildings, 2017).

Lu, Shen, Yao, & Wu (2005), argue that construction is the main source of environmental pollution compared to other industries, on the other hand, Bravo (2011) points out that the construction sector generates 36% of CO_2 emissions, in the European Economic Community and that it is the industry that consumes the most energy, generates the most waste and uses 60% of the materials that are extracted on the continent.

It has been reported that very few private developers and contractors make efforts to consider the environment and take into account the recycling of construction materials and give more importance to completion time (Poon, Yu, & Ng, 2001).

The construction sector is very important in the development of a country as it contributes to generate basic welfare elements in a society by building bridges, roads, ports, railways, dams, power plants, industries, as well as housing, schools, hospitals; allowing the development of urban areas and the growth of cities (INEGI, 2009).

In the coming decades, much of Mexico's population growth will be urban. This means that the country will grow from 384 cities to 961 in 2030, where 83.2% of the national population will be concentrated and where the poor population will most likely predominate (UN-Habitat, 2017).

In the state of Sonora in 1990, 79% of the population lived in localities of 2 500 and more inhabitants. In 2020, that percentage was 87.13%, for a population of 3 million 304 thousand 011 inhabitants (see Figure 3), according to data published by INEGI (2020).
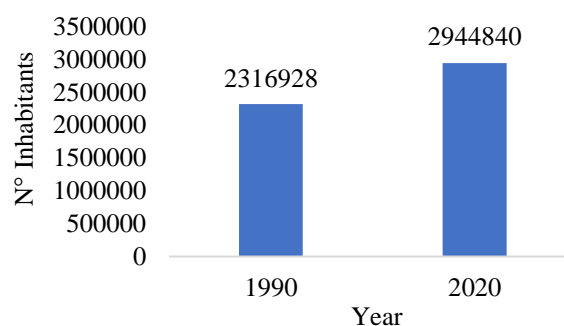
Figure 3 Urban population growth in Sonora
Source: INEGI, 2020

The state of Sonora has been characterised by demographic concentration, a product of migratory flows that have opted to seek alternatives for better jobs and income. First secondary activities and now tertiary activities have been the main attractions of these demographic movements, which have been lodged in certain points of the territory known as population centres. The advantages of location, as well as the density and speciality of non-primary activities, have led to different urbanisation phenomena in the territory.

This urbanisation process has also been characterised by intense land use measured by population density (Sidur, 2016). All this will increase the distances, times and costs of urban journeys, and will require increased investment to achieve greater connectivity between workplaces and housing or service centres.

Urban spaces can be defined as areas accessible to all inhabitants and users at any time, they are composed of various structures that favour economic, social, cultural and any other activities of interest within the existing population, such an environment is mainly connected by a system consisting mainly of asphalt pavements of flexible type (asphalt binder) and/or rigid (hydraulic concrete); which, thanks to urban expansion, has become a growing social demand as an indicator of a better quality of life, thus generating a greater amount of resources for its construction, which in turn causes a greater impact on the environment (Cruz, Gallego, & González, 2009).

Urban pavements are made up of a pavement generally made up of several successive layers supported on the esplanade or embankment, which consists of a firm support surface with sufficient strength to withstand the stresses of the upper layers of the pavement during its construction and operation. The thickness of each of the three elements that make up external urban pavements (road surface, pavement and surface course) is determined according to the function for which the pavement is intended, the load and frequency of use that the pavement is intended to receive, and other particular desirable characteristics (Francalacci, 2010). Normally, urban pavements of the flexible hot mix asphalt type are made up of 4 layers consisting of the graded or embankment, the pavement, which in turn is made up of a sub-base, a base and the overlay represented, in this case, by an asphalt layer (see Figure 4).

Wearing course

Granular Base Course

Granular sub-base course

Embankment layer

Figure 4 Flexible pavement structure
Source: UNAM, 2018

According to Angulo and Zavaleta (2021), one option for the design of pavement structures is soil stabilisation, defined as the improvement of the physical properties of a soil through mechanical procedures and the incorporation of natural or synthetic chemical products. Soil stabilisation for roads has technical, environmental, economic and social advantages over traditional construction.

From the environmental point of view, the use of existing materials on the ground reduces the consumption of aggregates, reducing the exploitation of aggregate pits and riverbeds, and the transport of materials to and from the construction site, with a lower consumption of fossil fuels and emission of gases into the atmosphere.

It also has associated benefits for rural communities or populations, given that it is a faster construction technique than the traditional one, which implies shorter intervention times for roads, less presence of machinery in the environment and a positive perception of the environment.

In the world, the alternative of using geosynthetics is already common in many countries, where geogrids in flexible pavements increase the bearing capacity of a given material, providing lateral confinement, reducing the load stresses produced by vehicles on the pavement structure. These geogrids provide increased strength, which certifies a 90% higher efficiency (Tolentino, 2021).

At present, the carbon emissions or emission factors generated by each material, product or existing service are known, which has allowed us to clearly know the impact generated in each activity, allowing us to quantify the CO_2 emissions generated in the construction of a road infrastructure and how this can vary depending on the materials and the construction area, so it is imperative to consider the environmental impact generated by any construction (Rico, et al, 1998).

Different methodologies and tools are known to help us for the inventory of pollutant emissions both for organisations and for products or services in particular, with differences in terms of scope, gases covered or the scale to which it is applied.

So to select a methodology it is necessary to focus mainly on the objective that is planned to be obtained to achieve the expected result. Among the most widely used tools is the "Life Cycle Assessment" (LCA) which has been considered one of the most appropriate methodologies for the interactive study between products and services of the construction industry and the environment, as numerous objectives and methodological references have been used for its development (Naked, et al, 2013).

The LCA allows determining the environmental burdens associated with products, processes or activities (Condeixa, Haddad, & Boer, 2014), and is developed through the identification and quantification of energy, materials used and waste discharged into the environment (Domínguez & Júarez, 2011). Due to its simplicity, ease and efficiency, it has been used as a basis for various methodologies, tools and standards.

According to the "ISO 14040" standard, LCA is defined as a technique for determining the environmental aspects and potential impacts associated with a product (or service) through an inventory of the relevant inputs and outputs of the system, an assessment of the potential environmental impacts associated with those inputs and outputs, and an interpretation of the results of the inventory and impact phases in terms of the objectives of the study (Suárez, 2014).

LCA is a tool for a better understanding of the dimensions of the environmental profile of products, processes and services and is suitable for comparing the potential environmental impacts of two or more similar products and if necessary can be combined with economic and social considerations, and depending on the processes covered by the LCA, it can have different scopes, according to Badilla, et al. (2015).

– "Cradle to grave": Includes the extraction of raw materials and the processing of materials necessary for the manufacture of the component, the use of the product and finally its recycling and/or final management. Transport, storage, distribution and other intermediate activities between life cycle phases are also included when they are sufficiently relevant.

– "Cradle to gate": The scope of the system is limited from when raw materials are sourced to when the product is placed on the market, at the exit of the manufacturing plant.

– "From the door to the door": Only manufacturing processes are considered

There are various technologies for the determination of quantifications of greenhouse gas emissions and other environmental impacts, so-called specialised software or tools, among which we can find the software "Air.e HdC" which is focused on the calculation of Carbon Footprint of products, services, events, organisations and projects, allows the preparation of verification reports and is adjusted to the international standards ISO 14040, PAS 2050, GHG Protocol, ISO 14064, ISO 14067 and ISO 14069 (TYS Magazine, 2014).

SimaPro" is an analytical software used to measure the environmental footprint of products and services in an objective way and with a high level of transparency and allows to view complete supply networks and provides a total view of databases and unit processes, this provides full ability to analyse and modify choices and assumptions, indispensable for professional LCA investigations (SimaPro, 2017). In relation to the existence of previous works carried out by various researchers having carbon footprint and the construction industry as a topic we find the following:

Environmental impact assessment of outdoor urban pavements (Francalacci, 2010). Environmental impact of road projects. Effects of the construction and maintenance of road surfaces: II rigid pavements. (Hernández, et al, 2001). Model for quantifying the CO_2 emissions produced in buildings derived from the material resources consumed in their execution (Mercader, Ramírez, & Olivares, 2013).

Assessment of the Carbon Footprint with a Life Cycle Analysis approach for 12 Building Systems (Güereca, et al, 2016). Determination of the carbon footprint in the construction of 3 types of Walls, applied to low-income housing, Mexico-Puebla (Hoyos, 2018).

In the same way, the research analysed various existing methodologies for calculating the carbon footprint or CO_2 emissions, some of which were, Methodologies for calculating the carbon footprint and its potential implications for Latin America (ECLAC, 2010). 7 methodologies for calculating greenhouse gas emissions (IHOBE, 2013). Methodological approaches for calculating the carbon footprint (Herrero, 2017).

In the present project, the carbon footprint of an asphalt pavement is calculated in kg CO_2 eq per m^2 in Ciudad Obregón Sonora, Mexico, by means of emission factors obtained from Simapro 9.0 software, with the Ecoinvent 3 libraries. Allocation at point substitution system APOS U- used in this LCA project, Method Global, ReCiPe 2016 Midpoint (E), World 2010 E, option characterisation, taking into account from the process of obtaining the raw material to the production of inputs, in the machinery the operation of the equipment is taken into account, as well as that of fuels and oils.

The object of the study was considered to be the functional unit $1m^2$ of asphalt pavement of 4 cm thickness, 15 cm thickness of the base layer, 15 cm thickness of the sub-base layer and 20 cm thickness of the underlying layer as natural soil material.

It was hypothesised that the emissions in KG-CO_2/m^2 produced by the asphalt binder pavements are within the range of 10-25 KG-CO_2/m^2, and that the emissions in KG-CO_2/m^2 produced by the asphalt binder pavements are within the range of 10-25 KG-CO_2/m^2

Methodology

Participants:

–   Research professor of the Instituto Tecnológico de Sonora of the Civil Engineering Department, who created the main idea of the project, as well as the research guide and provided the tools and means for it.

–   Students from the Civil Engineering educational programme of the Sonora Institute of Technology, who helped in the collection of information and preliminary tests of the SIMAPRO 9.0 software, with the aim of developing them to continue the research with other types of works or pavements.

Materials and equipment:

–   Paving plans of the subdivision: File where the shape, dimensions and design characteristics are specified.
–   Equipment: Desktop computer and LAP TOP.
–   AutoCAD, Software for the design, revision and modification of plans.
–   OPUS 2010 software, for the determination of fuel consumption of the equipment.
–   Microsof, Word, Excel and PPT.
–   Earth Google, for the location of the subdivision and the distances to the places of origin of the materials.
–   The SIMAPRO 9.0 software was used to determine the CO_2 emissions (carbon footprint) in Kg-CO_2 eq, which is based on the Life Cycle Analysis (LCA) methodology and has as its regulatory framework the international standards of application such as:

    –   UNE-EN ISO 14040.
    –   UNE-EN ISO 14044.

Several tables were designed in Excel and formulated for the capture of project data to determine the quantities of work for each layer of the structure, to quantify the number of working hours and the number of litres of fuel (diesel) consumed at each stage of the construction process.

Design of tables to calculate the quantities of work per functional unit m2 of pavement indicating each layer of the structure, which included base materials, sub-base, sub-surface and asphalt binder, as well as the watering and impregnation, also the tables of volumetric weights that allowed to convert the units of weight to mass and to be able to use it in mass units as allowed by the software Simapro 9.0.

Procedure:

1. Once the object of study has been selected, and all its characteristics are known:

– Location
– Plans and projects
– The content of the projects relating to the layout, road area, characteristics of the pavement structure (thickness of the different layers of asphalt binder, base, sub-base and underlayer).
– Location of procurement points for the various materials required in the different stages or layers of construction in relation to the location of the subdivision.

2. In relation to the construction site and construction processes:

– Defined the various activities required for each layer of the pavement structure and the appropriate equipment.
– Calculated the volumes or quantities of work at each stage of the construction process relating to the various layers that make up the pavement structure.
– Calculated the consumption in litres of fuel per HP of equipment power per hour of work, considering the operating factors.
– Designed tables to calculate the quantities of work per functional unit m2 of pavement indicating each layer of the structure, which included base, sub-base, sub-surface and asphalt binder materials and the binding and impregnation watering.
– The volumetric weight tables were established to convert the weight units to mass and to be able to use them in mass units as allowed by the SIMAPRO 9.0 software used.

3. Procedures for data collection:

– The information on CO_2 emissions were those established in the software available for the SIMAPRO 9.0 project.

Results

In this work there are two types of results, preliminary and necessary for the development of the study and the final results relating to the carbon footprint.

Figure 5 shows how the inputs to the construction process behaved, the process itself in its development and its outputs, in which the materials, energy consumption of the construction work and the transport of materials to the site stand out, and a square metre of pavement with a defined structure was also established as a functional unit.
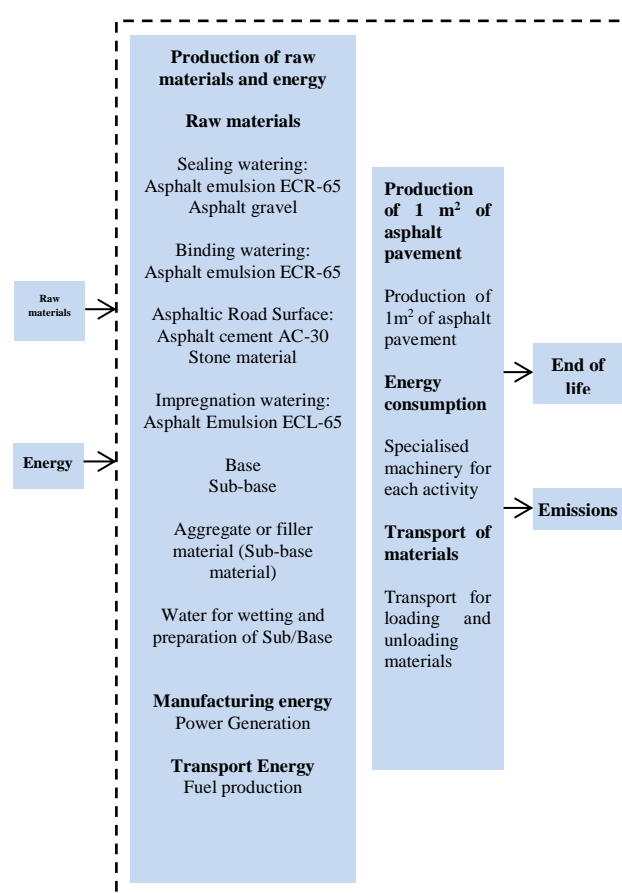
Figure 5 Schematic of the product-system
Source: Own Elaboration

Figure 6 shows the pavement structure where the thickness of the asphalt layer is 4 cm thick.
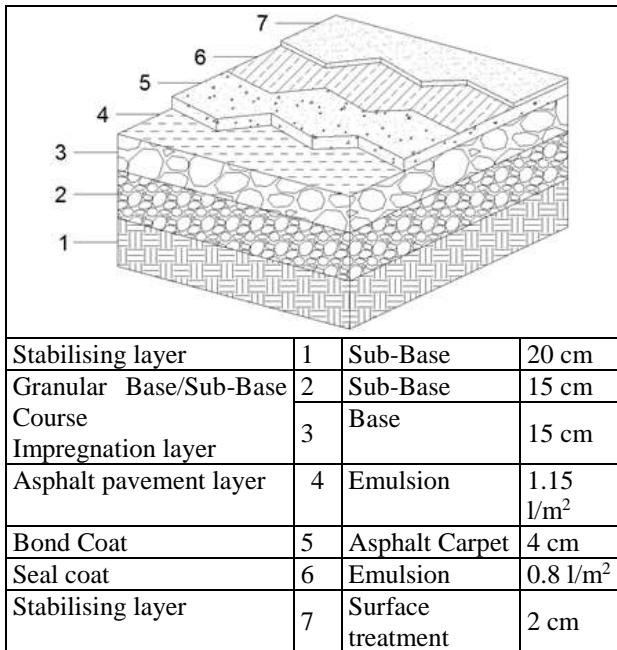
Stabilising layer	1	Sub-Base	20 cm
Granular Base/Sub-Base	2	Sub-Base	15 cm
Course Impregnation layer	3	Base	15 cm
Asphalt pavement layer	4	Emulsion	1.15 l/m²
Bond Coat	5	Asphalt Carpet	4 cm
Seal coat	6	Emulsion	0.8 l/m²
Stabilising layer	7	Surface treatment	2 cm

Figure 6 4 cm asphalt pavement structure specifications
Source: Own Elaboration

In table 1, the materials can be seen, where the subgrade stands out with 488,580 kg, the base and subbase with 312,475 kg, and the lowest values are for the cementitious material and asphalt emulsion with 1,574 and 1,229 kg respectively.

Material	Ud.	Cant. (m³)	Specific gravity (kg/m³)	Conversion (kg)
Sub-Base	m³	0.2874	1700.00	488.580
Sub-Base	m³	0.2155	1450.00	312.475
Base	m³	0.2155	1450.00	312.475
Stone material	m³	0.0553	1500.00	82.950
Asphalt gravel	m³	0.0276	1500.00	41.400
Asphalt cement AC-30	m³	0.0015	1035.27	1.574
Asphalt emulsion ECR-65	m³	0.0024	1001.59	2.424
Asphalt emulsion ECL-65	m³	0.0012	1015.88	1.229
Water	m³	0.1260	1000.00	126.000

Table 1 Volumes and weights of materials at fractionation Real de Sevilla III 4 cm
Source: Own Elaboration

In the analysis of the emissions generated by the transport of inputs, the most unfavourable distances from the place where the inputs were obtained to the location of the fractionation were calculated, considering adequate transport for the transfer of each input, asphalt cement travels 1854.60 km, water, 9.00 km and stone material 35.70 km (see Table 2).

Material	Net distance to the activity site in km
Base	15.5
Sub-Base	15.5
Asphalt cement AC-30	1854.6
Stone material	35.7
Asphalt emulsion ECR-60 for the seal course	1854.6
Asphalt gravel	25.3
Asphalt emulsion ECL-65 for impregnation irrigation	1838
Asphalt emulsion ECR-60 for the binder irrigation	1838
Water	9

Table 2 Travel distances of materials to the Real de Sevilla III subdivisión
Source: Own Elaboration

Table 3 shows the quantities of diesel required in each of the stages of the construction process by the unit corresponding to each stage, where it is found that the sub-base works and the improvement of the compacted base require 0.4948 l/m³, while 0.0721 l/m³ are required for the asphalt layer.

Concept	Area	Vol. hauling (m3)	Vol. (m3)	Rend. (m³/hr)	Working hours	Pot.	l/hr	Factor de oper.	Diesel consumption (L)	Consumo diesel (L/m3)
Asphalt road surface		4469.10	5645.18	227.84	19.62	125	0.20	0.83	407.02	
Totals					19.62				407.02	0.0721
Base compc. Al 95%		16119.9	20955.9							
Extend		16119.90		268.00	60.15	125	0.20	0.83	1248.09	
Moisten		16119.90		200.00	80.60	205	0.20	0.83	2742.80	
Mix		16119.90		268.00	60.15	125	0.20	0.83	1248.09	
Extend		16119.90		268.00	60.15	125	0.20	0.83	1248.09	
Compact		16119.90		59.90	269.10	100	0.20	0.83	4466.99	
Totals					530.15				10954.06	0.5227
Sub-Base compc. al 95%		16972.30	23225.25							
Extend		16972.30		227.84	74.49	125	0.20	0.83	1545.75	
Moisten		16972.30		200.00	84.86	205	0.20	0.83	2887.84	
Mix		16972.30		268.00	63.33	125	0.20	0.83	1314.09	
Extend		16972.30		268.00	63.33	125	0.20	0.83	1314.09	
Compact		16972.30		63.59	266.90	100	0.20	0.83	4430.57	
Totals					552.91				11492.34	0.4948
Impregnatio n irrigation	107466.24			15000	7.16	205	0.20	0.83	243.81	
Seal irrigation	107466.24			15000	7.16	205	0.20	0.83	243.81	
Totals					14.32				487.62	0.0045
Sub-grid improvement		21493.20	29411.75							
Extender		21493.20		227.84	94.34	125	0.20	0.83	1957.49	
Moisten		21493.20		200.00	107.47	205	0.20	0.83	3657.07	
Mix		21493.20		268.00	80.20	125	0.20	0.83	1664.12	
Extend		21493.20		268.00	80.20	125	0.20	0.83	1664.12	
Compact		21493.20		63.59	338.00	100	0.20	0.83	5610.74	
Totals					700.21				14553.54	0.4948
Dompe seal installation	107466.24		0.00	15000	7.16	175	0.20	0.83	208.13	
Laying of gravel with dompe	107466.24		29411.75	125.00	17.19	100	0.20	0.83	285.43	
Totals					24.35				493.56	0.0046
Totals					1841.57				38388.11	

Table 3 Machinery working hours and fuel consumption for each stage of the construction process in the Real de Sevilla III subdivision
Source: Own Elaboration

Table 4 shows the quantities of calorific value for the functional unit of one m² of the Real de Sevilla III subdivision, highlighting the volume of Sub-Base with a value of 17.790 MJ and the compacted base with 18.790 MJ, the lowest value is the impregnation irrigation with 0.165 MJ.

| Phase	MJ
Asphalt road surface	2.590
Compacted Base	18.790
Sub-base volume	17.790
Irrigation impregnation with oiling machine	0.163
Improvement of sub-base layer	17.790
Compaction of gravel with smooth compactor	0.165

Table 4 Real bridging fractionation calorific value in mj/m^3/phase
Source: Own Elaboration

Once the information necessary to use the Simapro software was gathered, the requested information was entered and the program was run.

The following results were obtained:

Figure 7, indicates in what percentages with which the different stages of the construction process contribute to the environmental impacts such as the case of the Sub-base with 33.30% and 32.04% of the base and in a sub-stage the burnt diesel fuel contributes 46.91%.
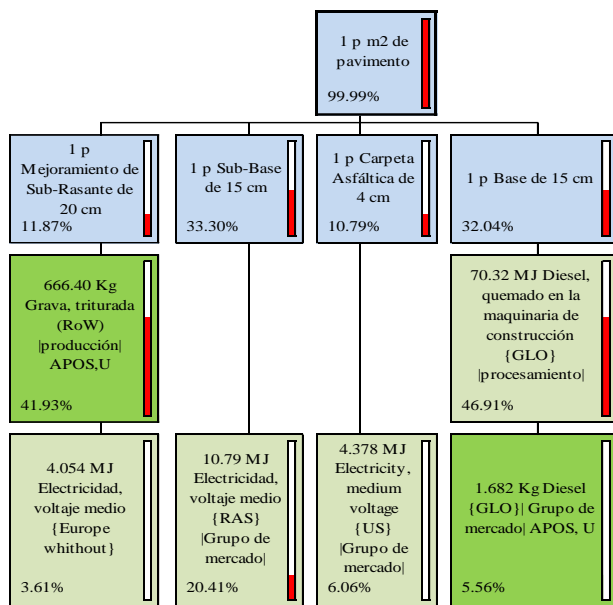
Figure 7 Contributions of the stages of the construction process and of the most representative materials involved Real de Sevilla III 4 cm Simapro 9.0
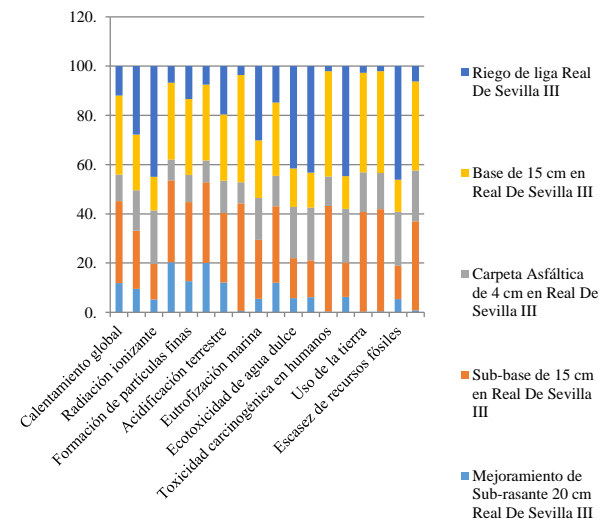*Source: Own Elaboration*

Table 5 shows the environmental impact categories, where it can be seen that global warming has a value of 12,618 kg CO_2 eq, of which the sub-base contributes 4,202 and the base 4,043 kg CO_2 eq, the values for ionising radiation are 2,403 kg CO_2, which is also a significant value.

Impact category	Unit	Total	Subgrade 20 cm	Subbase of 15 cm	Asphalt road surface of 4 cm	Base of 15 cm	Irrigation
Global warming	Kg CO₂ eq	12.618	1.498	4.202	1.361	4.043	1.514
Stratospheric ozone depletion	Kg CFC11 eq	1.33E-05	1.30E-06	3.20E-06	2.20E-06	3.00E-06	3.70E-06
Ionising radiation	KBq Co-60 eq	2.403	0.127	0.344	0.522	0.331	1.079
Terrestrial acidification	Kg SO2 eq	0.073	8.85E-03	0.021	0.010	0.020	0.014
Freshwater eutrophication	Kg P eq	3.26E-04	1.80E-06	1.42E-04	2.81E-05	1.42E-04	1.18E-05
Marine eutrophication	Kg N eq	3.50E-05	1.90E-06	8.40E-06	6.00E-06	8.20E-06	1.05E-05
Terrestrial ecotoxicity	Kg 1,4-DCB	10.412	1.248	3.242	1.275	3.110	1.537
Freshwater ecotoxicity	Kg 1,4-DCB	0.010	5.80E-04	1.62E-03	2.08E-03	1.56E-03	4.15E-03
Marine ecotoxicity	Kg 1,4-DCB	132.079	8.159	19.645	28.361	18.779	57.136
Human carcinogenic toxicity	Kg 1,4-DCB	2.045	7.29E-03	0.876	0.244	0.876	0.042
Land use	m²a crop eq	0.215	5.86E-04	0.087	0.034	0.087	5.84E-03
Scarcity of mineral resources	Kg Cu eq	4.82E-03	2.32E-05	2.00E-03	7.08E-04	1.99E-03	9.87E-05
Scarcity of fossil resources	Kg oil eq	9.651	0.519	1.299	2.132	1.244	4.457
Water consumption	m³	0.313	2.39E-03	0.113	0.065	0.113	0.020

Table 5 Emissions results and others by impact category 4 cm pavement of the Real de Sevilla III 9.0 subdivision
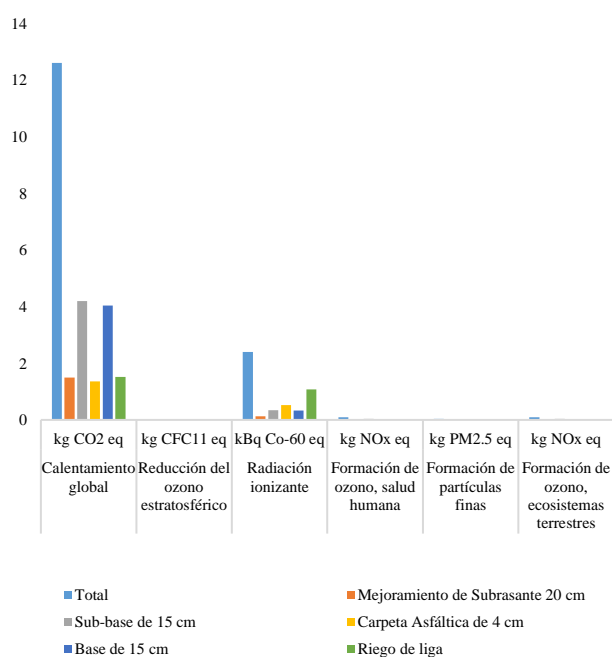*Source: Own Elaboration*

Figure 8 shows the results of the different environmental impacts and shows the 5 stages of the construction process in the category of global warming, the stages that contribute most are the sub-base and the base, in the same situation as occurs with ozone formation, on the other hand, in the category of freshwater ecotoxicity and marine ecotoxicity, the stage that contributes most is the irrigation stage.

Figure 8 Graph of the categories of environmental impacts in the different stages of the construction process in the Real de Sevilla III 4 cm Simapro 9.0 subdivision
Source: Own Elaboration

Figure 9 shows that CO_2 emissions related to global warming are the most representative of the construction process and are in the order of 13 kg of CO_2, it is also observable that the stages that contribute the most are the base and sub-base, another of the categories that stands out is ionising radiation in KBqCO-60eq, which is in the order of 1.5 kg, where it can be seen that the stage that contributes most is the stage of irrigation of the asphalt emulsion.

Figure 9 Categories of environmental impacts associated with greenhouse gas emissions from the 4 cm pavement of the Real de Sevilla III subdivision Simapro 9.0
Source: Own Elaboration

Table 6 shows the final results where the emissions in kg CO_2 eq/m^2 are 12.618 while the totals correspond to a total area of 90,418.33 m^2 of asphalt paving construction which produces a total of 1,140,863.493 kg CO_2 eq.

Impact category	Global Warming	Paved area	Emissions in kg-CO₂/fracking
Unit	kg de CO_2 eq/ m^2	m^2	kg de CO_2 eq
Layer of 4 cm	12.618	90, 418.33	1, 140, 863.69
Total		90,418.33	1, 140,863.69

Table 6 Analysis Emissions in Kg- CO_2 eq./m^2 generated in the Real de Sevilla III subdivisión
Source: Own Elaboration

Conclusions

The tables and figures above were used to determine the final conclusions of this work.

1. Emissions in kg of CO_2 eq/m2 are 12.618 while the totals correspond to a total area of 90,418.33 m^2 of asphalt pavement construction.

2. Hypothesis raised for the study states textually the following: "Hi: In the construction of a flexible pavement in a subdivision in Ciudad Obregón Sonora, between 10 and 25 kgCO_2/m^2 are emitted", so it can be concluded that the hypothesis is accepted since the value found is 12.618 Kg-CO_2/m^2, and it is within the proposed values.

3. Of the stages of the construction process, the contributions of emissions in kg of C O_2 eq/m^2, the highest contribution is the sub-base layer with 33.30%, while the lowest is the asphalt layer with 10.79%.

4. The highest Global Warming value corresponds to the sub-base with a value of 4,202 kg C O_2 eq/m^2, while the lowest value is for the asphalt layer with 1,361 kg CO_2 eq.

5. The total emissions of the subdivision are 1,140,863.493 kg CO_2 eq.

6. If these values are to be reduced, lime stabilisation techniques for base and sub-base materials can be used, which can reduce the need for base and sub-base materials and eliminate the need to carry them.

Recommendations

1. Taking into account that the durability of the flexible pavement and according to Wright and Dixon, the climate and environment where a flexible pavement will be built, influences its useful life and it is very likely that two of the most influential factors are temperature and humidity, since under these conditions the flexible pavement has an average useful life of 12.5 years and taking into account that it has a higher maintenance cost and with a greater environmental impact when performing maintenance, it is recommended not to build with asphalt binder.

2. As the greatest contamination is generated in the movement of earth, it is advisable to explore the possibility of using the technique of soil stabilisation with lime, especially in the case of expansive clays, which are very common in our environment.

3. According to the development of our study, which indicates that a rigid pavement "are those that are fundamentally constituted by a hydraulic concrete slab, supported on the subgrade or on a layer, of selected material, which is called sub-base" this indicates that we can suppress one of the layers that most pollute the base in both results are contributing with values close to 30% of the total emissions of KG-CO$_2$ eq.

4. In rigid pavements, use ecological cement, which generates less Kg-CO$_2$/tonne emissions in its production process.

5. Carry out a greater number of studies changing the pavement variables, such as concrete, clay stabilisation, cobblestones, paving stones, soil cement.

References

Acosta , B. (2019). *Qué es la gestión ambiental*. Recuperado el 2020, de Ecologia verde: https://www.ecologiaverde.com/que-es-la-gestion-ambiental-2035.html

Acosta, D. (2002). *Reducción y Gestión de Residuos de Construcción y Demolición (RCD)*. Obtenido de Builders Guide: https://issuu.com/nelianaduran/docs/reciclaje_de_materiales_de_escombro_9ce808e173be90

Angulo, R., & Zavaleta, P. (2021). *Estabilización de suelos arcillosos con cal para el mejoramiento de las propiedades fisico–mecánicas como capa de rodadura en la prolongación Navarro*. Recuperado el 2021, de Distrito San Juan–Maynas–Iquitos: http://repositorio.ucp.edu.pe/bitstream/handle/UCP/1220/ANGULO%20ROLDAN%20MARISELVA%20Y%20ZAVALETA%20PAPA%20CINTIA%20NICOL%20-%20TESIS.pdf?sequence=1&isAllowed=y

Aparicio, P. (2020). *Caracterización de impactos ambientales en la industria de la construcción*. Obtenido de 360° en Concreto: https://www.360enconcreto.com/blog/detalle/impactos-ambientales-en-la-industria-de-la-construccion

Arenas, F. (1 2010). *Los materiales de construcción y el medio ambiente*. Recuperado el 2019, de ESTUDIOS: https://huespedes.cica.es/gimadus/17/03_materiales.html

Badilla , P., Elizondo , J., Fernández, T., Mora, F., Méndez, J., & Quesada , M. (2015). *CO2e: cálculo de huella de carbono para materiales de construcción en Costa Rica*. Obtenido de Redalyc: http://repositorio.sibdi.ucr.ac.cr:8080/jspui/handle/123456789/3212

Bravo, R. (2011). *El sector de la construcción genera el 36% de las emisiones de CO2 en la Unión Europea*. Obtenido de dicyt : http://www.dicyt.com/noticias/el-sector-de-la-construccion-genera-el-36-de-las-emisiones-de-co2-en-la-union-europea

CEPAL. (e 2010). *Metodologías de cálculo de la Huella de Carbono y sus potenciales implicaciones para América Latina*. Recuperado el 07 de 06 de 2020, de CEPAL: https://www.cepal.org/es/publicaciones/37288-metodologias-calculo-la-huella-carbono-sus-potenciales-implicaciones-america

Cidead. (2018). *La humanidad y el medio ambiente*. Obtenido de Cidead: http://recursostic.educacion.es/secundaria/edad/4esobiologia/4quincena12/Contenidos/pdf_q12.pdf

Condeixa, K., Haddad, A., & Boer, D. (2014). *Life Cycle Impact Assessment of masonry system as inner walls: A case study in Brazil*. Recuperado el 24 de 04 de 2020, de Construction and Building Materials: http://dx.doi.org/10.1016/j.conbuildmat.2014.07.113

Cruz, V., Gallego, E., & González, L. (12 de 08 de 2009). *Sistema de evaluación de impacto ambienta*. Recuperado el 2020, de Universidad Complutense de MADRID : https://eprints.ucm.es/9445/1/MemoriaEIA09.pdf

Domínguez, J., & Júarez, M. (2011). Inventarios para Análisis del Ciclo de Vida de Materiales para la Construcción en el Sureste de México. *CILCA*, 42-44.

Encinas, M. (2011). *Medio Ambiente y Contaminación. Principios Básicos* . Obtenido de ADDI: https://addi.ehu.es/bitstream/handle/10810/1678 4/Medio%20Ambiente%20y%20Contaminaci% C3%B3n.%20Principios%20b%C3%A1sicos.p df?sequence=6&isAllowed=y

Florides, G., Christodoulides, P., & Messaritis, V. (2013). *Reviewing the effect of CO 2 and the sun on global climate.* Obtenido de Renewable and Sustainable Energy reviews: http://www.sciencedirect.com/science/article/pi i/S1364032113003651

Francalacci, B. (2010). *Evaluación del impacto ambiental de los pavimentos urbanos exteriores.* Obtenido de Universitat Politècnica de Catalunya: https://wwwaie.webs.upc.edu/maema/wp-content/uploads/2016/07/07-Beatriz-Francalacci-da-Silva-Evaluacion-del-impacto-ambiental-de-los-pavimentos-urbanos-exteriores_COMPLETO.pdf

Growing Buildings. (2017). *Construcción y emisiones CO2 a la atmósfera*. Obtenido de Growing Buildings: https://growingbuildings.com/construccion-y-emisiones-co2-a-la-atmosfera/

Güereca, L., Padilla, A., Herrera, H., & Carius, C. (2016). *Evaluación de la Huella de Carbono con enfoque de Análisis de Ciclo de Vida para 12 Sistemas Constructivos.* Obtenido de UNAM: http://www.novaceramic.com.mx/pdf/emisiones _co2.pdf

Hernández, J., Sánchez, V., Castillo, I., Damián, S., & Téllez, R. (2001). *Impacto ambiental de proyectos carreteros, efectos por la construccion y conservacion de superficies de rodamiento: II pavimentos rigidos.* Obtenido de SCT: https://www.imt.mx/archivos/Publicaciones/Pu blicacionTecnica/pt173.pdf

Herrero, J. (2017). *Enfoques metodológicos para el cálculo de la Huella de Carbono.* Recuperado el 07 de 06 de 2020, de OSE: http://www.carbonfeel.org/Carbonfeel_2/Bitaco ra/Entradas/2011/9/15_Informe_Enfoques_met odologicos_para_el_caclulo_de_la_Huella_de_ Carbono_del_Isntituo_de_la_Sostenibilidad_en Espana_files/Informe%20OSE.pdf

Hoyos, E. (2018). *Cuantificacion de la huella de carbono en la construccion de tres tipos muros, aplicado a casas de interes social en Mexico-Puebla.* Obtenido de Universidad de las Americas Puebla: http://catarina.udlap.mx/u_dl_a/tales/document os/lic/hoyos_de_la_vega_e/etd_401102660258 1.pdf

IHOBE. (2013). *7 Metodologías para elcálculodeemisiones degasesdeefectoinvernadero.* Recuperado el 2019, de EUSKADI: https://www.euskadi.eus/contenidos/documenta cion/7metodologias_gei/es_def/adjuntos/7MET ODOLOGIAS.pdf

INEGI. (2009). *Administracion de operaciones de construccion* . Obtenido de INEGI: https://www.inegi.org.mx/contenidos/saladepre nsa/boletines/2018/EstSociodemo/enh2018_05. pdf

INEGI. (2015). *Principales resultados de la Encuesta Intercensal 2015* . Recuperado el 2019, de INEGI : http://internet.contenidos.inegi.org.mx/contenid os/productos//prod_serv/contenidos/espanol/bvi negi/productos/nueva_estruc/inter_censal/estad os2015/702825079901.pdf

INEGI. (2020). *Censo de Población y Vivienda 2020.* Recuperado el 2021, de INEGI: https://www.inegi.org.mx/sistemas/olap/consult a/general_ver4/MDXQueryDatos.asp?#Regreso &c=

Intergovernmental Panel on Climate Change. (2007). *Cambio Climático 2007.* Obtenido de IPCC: https://www.ipcc.ch/site/assets/uploads/2018/02 /ar4_syr_sp.pdf

Intergovernmental Panel on Climate Change. (2014). *Vida Sostenible org.* Obtenido de Efectos Sociales del cambio Climático: http://www.vidasostenible.org/informes/consec uencias-sociales-del-cambio-climatico/

Lu, W. S., Shen, L. Y., Yao, H., & Wu, D. H. (2005). A computer-based scoring method for measuring the environmental performance of construction activities. *Automation in Construction*, 297-309.

Marino, D. (2009). *Estudio teórico experimental sobre respuestas biológicas a compuestos orgánicos de relevancia ambiental.* Obtenido de SEDICI: http://sedici.unlp.edu.ar/bitstream/handle/10915/2744/I_-_Introducci%C3%B3n_general.pdf?sequence=5

Medineckiene, M., Kazimieras , E., & Turskis, Z. (2010). *Sustainable Construction Taking into Account the Building Impact on the Environment.* Obtenido de Researchgate : https://www.researchgate.net/publication/228420911_Sustainable_Construction_Taking_into_Account_the_Building_Impact_on_the_Environment

Mercader, M., Ramírez, A., & Olivares, M. (2013). *Modelo de cuantificación de las emisiones de CO2 producidas en edificación derivadas de los recursos materiales consumidos en su ejecución.* Obtenido de CSIC: http://informesdelaconstruccion.revistas.csic.es/index.php/informesdelaconstruccion/article/view/2184

Naked, A., de Moraes, M., de Macedo, K., Evangelista, A., & Thomas , D. (2013). *Life Cycle Assessment: a Comparison of Ceramic Brick Inventories to Subsidize the Development of Databases in Brazil.* Obtenido de Applied Mechanics and Materials: www.scientific.net/AMM.431.370

OECC. (2014). *Guía para el cálculo de la huella de carbono y para la elaboración de un plan de mejora de una organización.* Obtenido de Oficina Española de Cambio Climático.: https://www.miteco.gob.es/es/cambio-climatico/temas/mitigacion-politicas-y-medidas/guia_huella_carbono_tcm30-479093.pdf

ONU. (2019). *Se alcanzan niveles récord de concentración de gases de efecto invernadero en la atmósfera .* Recuperado el 06 de 06 de 2020, de Noticias ONU: https://news.un.org/es/story/2019/11/1465851

ONU. (2020). *Informe sobre la brecha en las emisiones del 2020.* Recuperado el 2021, de Programa de las Naciones Unidas para el Medio Ambiente : https://wedocs.unep.org/bitstream/handle/20.500.11822/34438/EGR20ESS.pdf?sequence=35

ONU-Habitad. (2017). *Tendencias del desarrollo urbano en México.* Obtenido de ONU-Habitad: https://onuhabitat.org.mx/index.php/tendencias-del-desarrollo-urbano-en-mexico

Organización de las Naciones Unidas. (2019). *El aire Contaminado es un asesino peligroso.* Obtenido de Noticias ONU: https://news.un.org/es/story/2019/03/1452171

Poon, C., Yu, A., & Ng, L. (2001). *On-site sorting of construction and demolition waste in Hong Kong.* Obtenido de Conservation and Recycling: http://ira.lib.polyu.edu.hk/handle/10397/8748

Rico, A., Mendoza, A., Téllez, R., & Mayoral, E. (1998). *Algunos aspectos comparativos entre pavimentos flexibles y rígidos.* Obtenido de IMP: https://imt.mx/resumen-boletines.html?IdArticulo=113&IdBoletin=37

Ripoll, O., & Del Cerro, I. (2007). *Carreteras y sostenibilidad.* MEXICO: Ingenieria viaria y ambiental .

Semanart. (2015). *Atmósfera .* Obtenido de Semanart: https://apps1.semarnat.gob.mx:8443/dgeia/informe15/tema/cap5.html

Semarnat. (2010). *Industria y medio ambiente.* Obtenido de Semarnat: http://dgeiawf.semarnat.gob.mx:8080/ibi_apps/WFServlet?IBIF_ex=D2_R_INDUSTRIA01_01&IBIC_user=dgeia_mce&IBIC_pass=dgeia_mce

Semarnat. (2012). *Informe de la situacion del medio ambiente en mexico.* Obtenido de Compendio de Estadísticas Ambientales indicadores clave y desmpeño ambiental: https://apps1.semarnat.gob.mx:8443/dgeia/informe_12/pdf/Informe_2012.pdf

Sidur. (2016). *Programa Sectorial de Infraestructura y Desarrollo Urbano Sustentables.* Obtenido de Sidur: http://estrategia.sonora.gob.mx/images/PSEEG/ NormatividadPMP/Sectoriales/PS-SIDUR-16-21-SON.pdf

SimaPro . (2017). *SimaPro .* Recuperado el 02 de 06 de 2020, de SimaPro : https://www.simapro.mx/

Soto, González, & Fernández. (2013). El cambio climático y sus efectos en la salud. *Revista Cubana de Higiene y Epidemiología*, 331-337.

Suárez, S. (2014). *Viabilidad ambiental del reciclaje del yeso.* Recuperado el 24 de 04 de 2020, de CONAMA 2014: http://www.conama11.vsf.es/conama10/downlo ad/files/conama2014/CT%202014/1896712000. pdf

Sunyer, J. (2010). *Promoción de la salud frente al cambio climático. GacSanit.* Recuperado el 2012, de Barcelona [Internet]: http://scielo.isciii.es/scielo.php?script=sci_artte xt&pid=S0213-91112010000200001&lng=es

Tolentino , H. (2021). *Geomallas biaxiales para mejorar la subrasante de bajo valor de soporte california de un pavimento flexible*. Recuperado el 2020, de Pucusana: file:///C:/Users/haceves/Downloads/Tolentino_ HK-SD%20(1).pdf

TYS Magazine . (21 de 05 de 2014). *Herramientas de cálculo para conocer la huella de carbono*. Recuperado el 05 de 06 de 2020, de TYS Magazine : https://www.tysmagazine.com/calculo-huella-de-carbono/

UNAM. (2018). *Problemáticas económicas del agua en México.* Obtenido de Ciencia UNAM: http://ciencia.unam.mx/leer/775/problematicas-economicas-del-agua-en-mexico

Article

Design and Construction of an ALD Reactor by Growth of Al₂O₃ Nanostructure Films

Diseño y construcción de un reactor ALD por crecimiento de películas de nanoestructuras de Al₂O₃

MONTES-GUTIERREZ, Jorge*[1], LOPEZ-GASTELUM, Ana, ROMO-GARCÍA, Frank and GARCIA-GUTIERREZ, Rafael*[1]

[1]*Physics Research Department. Universidad de Sonora. Rosales y Luis Encinas, Hermosillo, Sonora, 83000, México*
[2]*Department of Physics. Universidad de Sonora. Rosales y Luis Encinas, Hermosillo, Sonora, 83000, México*
[3]*Department of Physics, Engineering and Mathematics. Universidad de Sonora. Lázaro Cárdenas del Río No.100, Francisco Villa, Navojoa, 85880, México*

ID 1st Author: *Jorge, Montes-Gutierrez* / **ORC ID:** 0000-0002-3078-6548

ID 1st Co-author: *Ana, Lopez-Gastelum* / **ORC ID:** 0000-0003-1274-1431

ID 2nd Co-author: *Frank, Romo-García* / **ORC ID:** 0000-0003-1640-8767

ID 3rd Co-author: *Rafael, Garcia-Gutierrez* / **ORC ID:** 0000-0001-5030-326X

Abstract

Objective: This project focuses on designing, building and commissioning work the atomic layer deposition (ALD) reactor for Al₂O₃ ultrathin film, which it will be contain specific components and a system's own control unit. Methodology: The ALD reactor was designed under a system to minimize components, flow lines and connections; to reduce manufacturing costs, volume of precursors, among others. Currently, ALD reactors are expensive to sell, maintain and replace parts. The design and manufacture of the ALD reactor manufactured at the University of Sonora (UNISON) is based on the state art with sequential binary reactions of the precursors, for the proposal for the manufacture of solar cells. Contribution: It was possible to build and commission the ALD reactor for the deposition of ultra-thin films, with the characteristics of being reproducible and scalable, which makes it attractive for commercialization. The homemade ALD reactor at UNISON is considered a very interesting equipment for the semiconductor research area, since it is possible to combine different types of materials in the form of films such as oxides and nitrides in the order of Angstroms (Å).

ALD, Reactor, Thin films

Resumen

Objetivo: Este proyecto se centra en el diseño, construcción y puesta en marcha del reactor de deposición de capas atómicas (ALD) para película ultrafina de Al2O3, que contendrá componentes específicos y una unidad de control propia del sistema. Metodología: El reactor ALD fue diseñado bajo un sistema para minimizar componentes, líneas de flujo y conexiones; para reducir los costos de fabricación, volumen de precursores, entre otros. En la actualidad, los reactores ALD son caros en cuanto a su venta, mantenimiento y sustitución de piezas. El diseño y fabricación del reactor ALD fabricado en la Universidad de Sonora (UNISON) se basa en el estado del arte con reacciones binarias secuenciales de los precursores, para la propuesta de fabricación de celdas solares. Contribución: Se logró construir y poner en marcha el reactor ALD para la deposición de películas ultrafinas, con las características de ser reproducible y escalable, lo que lo hace atractivo para su comercialización. El reactor ALD casero de UNISON se considera un equipo muy interesante para el área de investigación de semiconductores, ya que es posible combinar diferentes tipos de materiales en forma de películas como óxidos y nitruros del orden de los Angstroms (Å).

ALD, Reactor, Películas finas

Citation: MONTES-GUTIERREZ, Jorge, LOPEZ-GASTELUM, Ana, ROMO-GARCÍA, Frank and GARCIA-GUTIERREZ, Rafael. Design and Construction of an ALD Reactor by Growth of Al₂O₃ Nanostructure Films. Journal of Technological Engineering. 2021. 5-16: 27-31

* Correspondence to Author (e-mail: rafael.gutierrez@unison.mx)
† Researcher contributing as first author.

Introduction

The atomic layer deposition (ALD) technique has its origin in Finland in 1974 by Toumo Suntola, et.al. and it is used for the growth of ultrathin films with high uniformity for multiple applications (T. Suntola, et.al. 1977). The state of the art of the ALD process involves a series of precursors which are released sequentially under controlled conditions of surface saturation of molecules available for anchoring in the substrate. The process is repetitive and sequential; therefore it is possible to control in more detail the thickness of the films with atomic precision. The incorporation of different precursors in the ALD system, favors the possibility of alternating several films of different materials (G. Steven M., 2010).
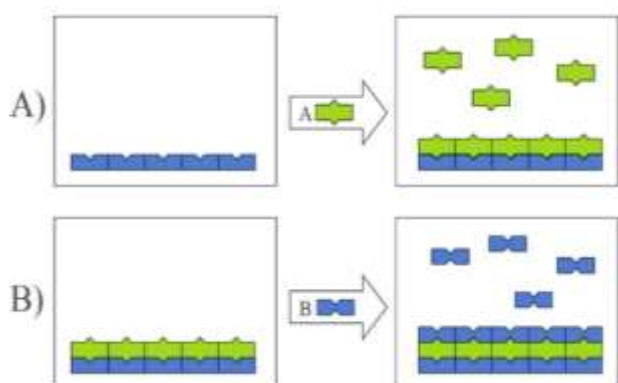
Figure 1 Atomic layer deposition (ALD) diagram

The figure 1 show the ALD diagram where is appreciable two precursors A and B creating two layers. First is deposited one layer with precursor A and when is saturated the remained is purged, the second layer is deposited with precursor B, and the same way the remained of precursor B are purged.

In recent years, the ALD technique has grown exponentially using in all semiconductor industries such as the manufacture of integrated circuits, sensors, micro and nanostructured electromechanical systems (MEMS and NEMS), optoelectronics, mechanics and renewable energy. Some examples of ALD applications are presented in protection against corrosion, energy production in solar cells, coatings of biological compatibility for medical devices and implants, water purification, OLED lighting devices, among others (H. Kim, et.al., 2009; Leskelä, M. and Ritala, M. 2003).

The ALD technique has advantages over other depositing techniques such as CVD or sputtering, having the ability to create ultrathin films with the ability to coat surfaces following irregular topographies (R. Johnson, et.al., 2014). The present work focuses on the design and construction of an ALD reactor with the characteristic of being reproducible, scalable and assembly for various chamber types, using coordinated ALD valves under a controller programmed with LabView2015.

Methodology to be developed
Materials and methods

a)   Materials

–   2-way and 3-way ALD valves
–   Bellows Valve
–   Cylinders for sampling
–   Thermal Tapes
–   Vacuum Sensor and Gauge
–   AALBORG GFC17 Mass Flowmeter
–   EDWARS RV3 Vacuum Pump
–   Temperature controllers
–   Computer
–   Arduino / Genuine Uno Hardware
–   12V 5A power supply
–   Bank of relays 5V, 10 A
–   LabVIEW 2015 programming software
–   Front panel
–   Precursors and reagents (TMG, TMI, TMA, NH_3 and Ar)

b)   Method

The ALD reactor was first designed under the specifications based on the state of the art of the art. The design was made in Solid Works to be presented and describe the operation from the flow of precursors to their incorporation into the surface of the substrate. (See figure 2).
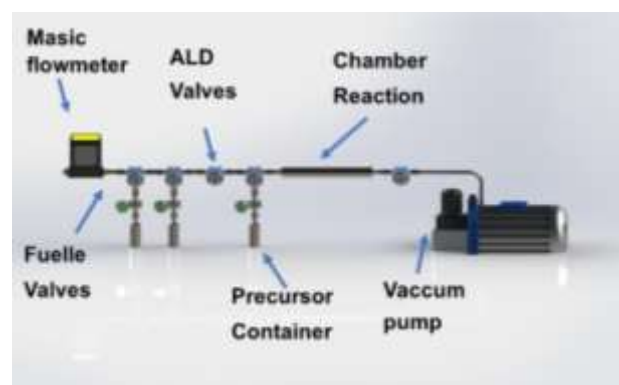
Figure 2 ALD system designed by SolidWorks

The ALD reactor has a series of assemblies ranging from a 100 sccm mass flow meter, bellows valves, ALD valves, several precursor container cylinders, the reaction chamber and a mechanical vacuum pump.

Subsequently, in figure 3 the electro-pneumatic and control design was carried out, which are in charge of controlling the work of opening and closing the ALD valves, both to release the precursors and for cleaning.
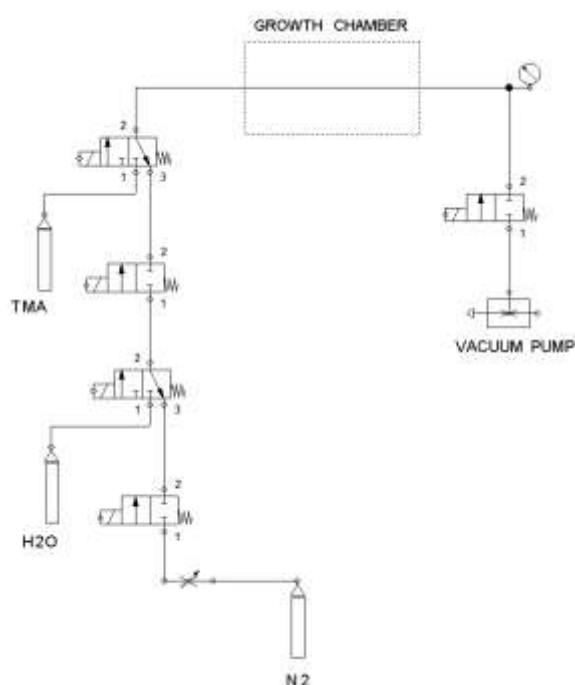
Figure 3 Electro-pneumatique designee of ALD system

The cabinet contains temperature controllers for thermal tapes, a microprocessor as an interface with LabVIEW that sequentially actuate the ALD valves, under set trip times with a bank of relays connected to a DC voltage source which feeds all the components.

In figure 4 show the LabVIEW programming was carried out at the user's disposal and is divided into two parts: a) control panel and b) block diagram. The block diagram develops the programming code for the manipulation and execution of the valve operation (number of cycles, exposure time of the precursor, reagents, purge gas, vacuum and an emergency button). An Arduino is integrated into the flow diagram as a data acquisition card.
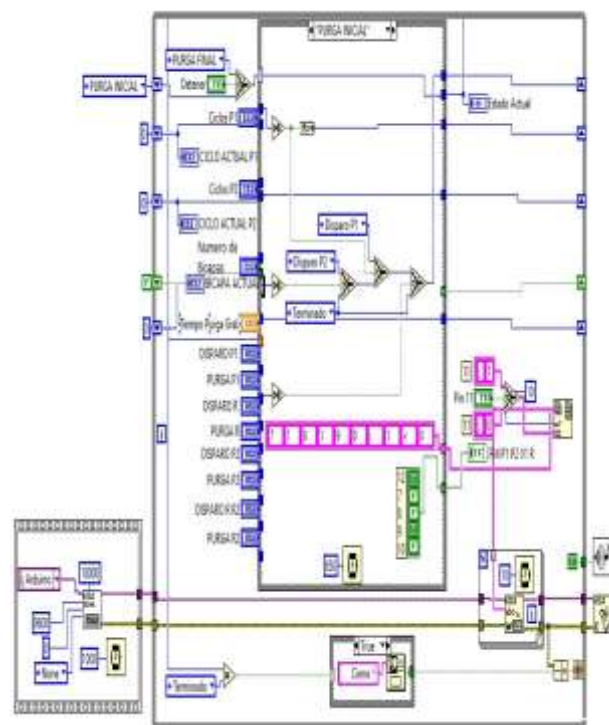
Figure 4 Block diagram developed with LabVIEW for the ALD reactor

Results

The ALD reactor was assembled from the mechanical parts, the electrical connections, gases and controllers, as well as the computer with which it has the software designed to send command programming and data capture. Figure 5 shows the ALD reactor with all its assembled components.

Figure 5 ALD reactor complete

The software has the programming commands of:

1. Purge time
2. Number of bilayers
3. Number of cycles
4. Precursor firing time
5. Purge time
6. Working times
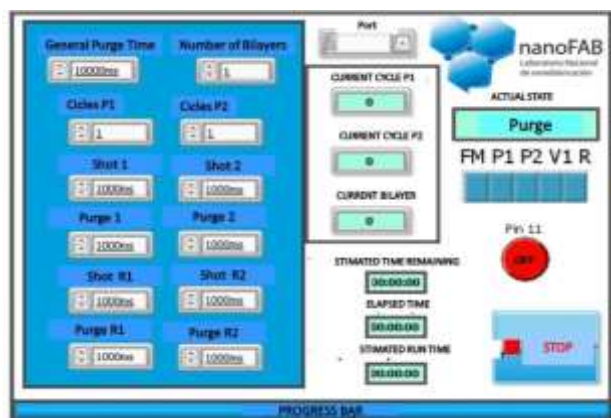7. Off button. (See figure 6).

MONTES-GUTIERREZ, Jorge, LOPEZ-GASTELUM, Ana, ROMO-GARCÍA, Frank and GARCIA-GUTIERREZ, Rafael. Design and Construction of an ALD Reactor by Growth of Al_2O_3 Nanostructure Films. Journal of Technological Engineering. 2021

Figure 6 ALD reactor control panel

A reactor workbook was described ALD, where its execution is summarized in 14 steps to process sample, which are the following:

A)   Sample introduction

1.   Fix substrate to sample holder
2.   Introduce it to the camera
3.   Reach the desired vacuum
4.   Opening of material valves

B)   Parameter settings

5.   Temperature in the 4 zones
6.   Number of cycles
7.   Shooting time

C)   AML process

8.   Initial purge
9.   Execution of ALD cycles
10.   Final purge

D)   Sample extraction

11.   Close material valves
12.   Lower temperature
13.   Ventilate with N2
14.   Take Samples

The results of handling the ALD reactor and the synthesis of ultrathin films are described below:

A) It was possible to deposit aluminum oxide (Al_2O_3) at two points in the reaction chamber. The experiment was carried out under 240 cycles, 200 °C in the reaction chamber, water and trimethyl-aluminum (TMA) as precursors and swept with N_2 flow.
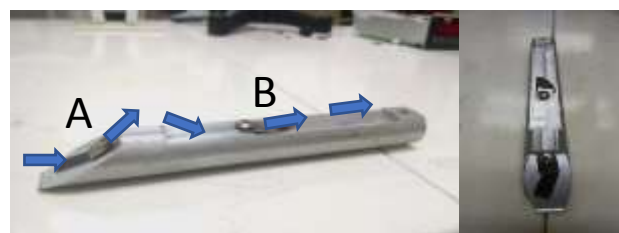

Figure 7 ALD substrate holder. Two locations of substrate A and B are shown. The flow of precursors sticks directly to substrate A and rebounds to substrate B

The films deposited on substrates A and B were analyzed by ellipsometry (Philips PZ2000, HeNe 632.8nm) obtaining the following averages of thicknesses obtained in 16 points

Sample	Thickness (nm)	Growth Range (Å/ciclo)
Sample A	29.4	1.22
Sample B	28.5	1.19
Differences	.9	.03

Table 1 Ellipsometry measurement of sample of substrate A and B

A topographic analysis was performed to analyze the uniformity of the thin film surface by plotting the 16 analysis points taken in ellipsometry using Wolfram Mathematica 9.0 software. (See figure 8).
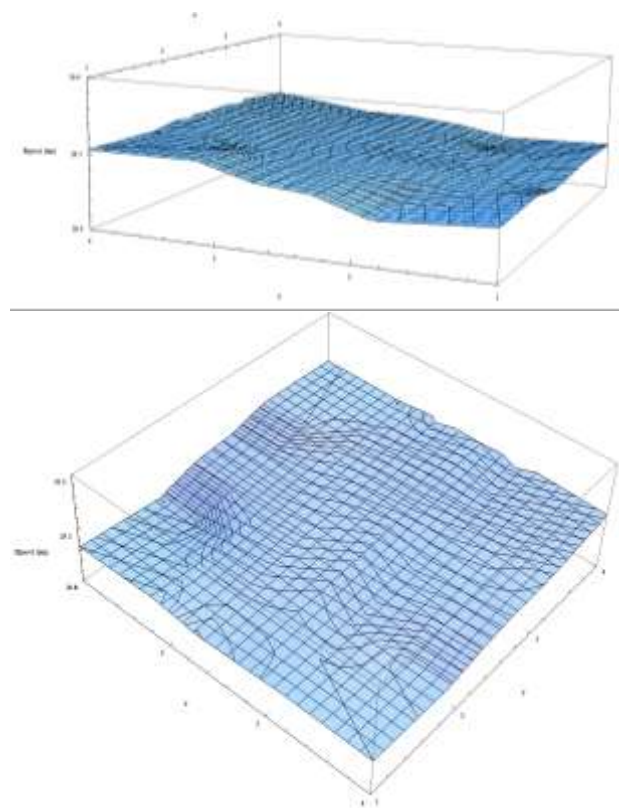

Figure 8 Topography graph of ALD de Al_2O_3 deposits

MONTES-GUTIERREZ, Jorge, LOPEZ-GASTELUM, Ana, ROMO-GARCÍA, Frank and GARCIA-GUTIERREZ, Rafael. Design and Construction of an ALD Reactor by Growth of Al_2O_3 Nanostructure Films. Journal of Technological Engineering. 2021

B) It was possible to deposit thin films of Al2O3 on nanoparticles (NP's) Si on a substrate of Si. The experiment was carried out at 40 cycles, 180°C in the reaction chamber, water and trimethyl-aluminum (TMA) as precursors and swept with N_2 flow.
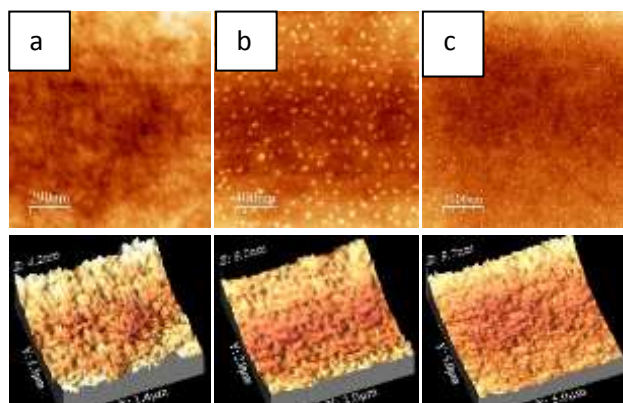
Figure 9 (a) Reference sample without ALD deposit of Al2O3, (b, c) silicon nanoparticle films subjected to 40 ALD cycles of alumina

Figure 9 shows atomic force microscopy (AFM) micrographs where the following samples are described: a) the deposit of Si NP's on a Si substrate. Images b) and c) show results of ALD deposits of Al_2O_3 / Si NP's / Si. In images a) and b) it is observed how the morphology of the Si NPs is maintained in the Al2O3 deposit, in a uniform way.

Acknowledgements

Conclusions

In this project, the objectives in the design, manufacture and start-up of an ALD reactor were met, with an efficient and high-precision system for thin-film deposits. This ALD reactor is fully reproducible and scalable which makes it perfect for commercial and industrial applications.

Likewise, the ALD reactor turned out to be an essential tool in the investigation of nanostructured materials by combining layers of thin films of different materials such as oxides and nitrides in the nanometer range and with the possibility of controlling ultrathin film thicknesses in the order of Ångströms.

The characteristics of this ALD system can lead to the discovery of new properties in semiconductor materials for application in optoelectronic devices such as high-efficiency solar cells and solid-state lighting.

References

George, Steven M. (2010). *Chem. Rev., 110 (1), 111 131*. doi: 10.1021 / cr900056b

Johnson, R. W.; Hultqvist, A., Doblado, S. F. (2014). Una breve revisión de la deposición de la capa atómica: de los fundamentos a las aplicaciones. Materials Today, 17 (5), 236–246. doi: 10.1016 / j.mattod.2014.04.026

Kim, H.; Lee, H. B. R.; Maeng, W. J. (2009). Applications of atomic layer deposition to nanofabrication and emerging nanodevices. Solid Films, 517, 2563.

Leskelä, M. and Ritala, M. (2003), Atomic Layer Deposition Chemistry: Recent Developments and Future Challenges. Angewandte Chemie International Edition, 42: 5548-5554. https://doi.org/10.1002/anie.200301652

T. Suntola, J. Antson, U.S. Patent 4,058,430, 1977.

Interactive assistant tool for the evaluation of kinematic patterns and EMG signals in patients with a forearm injury

Herramienta de asistente interactivo para la evaluación de patrones cinemáticos y señales EMG en pacientes con lesión del antebrazo

JIMÉNEZ-GONZÁLEZ, Fernando C.†* & TORRES-RAMÍREZ, Dulce Esperanza

Universidad Tecnológica de Ciudad Juárez

ID 1st Author: *Fernando C., Jiménez-González* / **ORC ID**: 0000-0002-4577-3408, **CVU CONACYT ID**: 443945

ID 1st Coauthor: *Dulce Esperanza, Torres-Ramírez* / **ORC ID**: 0000-0001-8409-2691, **Researcher ID Thomson**: U-8237-2018, **CVU CONACYT ID**: 322126

Abstract

Subjective feelings feedbacks are commonly employed by a patient during forearm rehabilitation therapy without real-time data, leading to suboptimal recovery results in some patients. Technological innovations in the field of assisted rehabilitation have enabled the evolution of real-time monitoring systems. In this paper, interactive assistant development is presented as the interface to define the relationship between the kinematics patterns and the electromyographic signals during the forearm rehabilitation routine. Leap Motion (LM) and Shimmer3 EMG sensors read the routine behavior by following the movements that appear on the software. Real-time targets are programmed to lead the necessary forearm movements that the therapist sets to determine the recovery progress. The integration of software and hardware shows a dataset basis on interaction variables such as arm velocity, arm position, performance rate, and electrical muscle pulse. The results obtained from tests show that the system works effectively within a range of movement of 9 to 88 degrees in rotation about the axes, and velocities under 190 mm/s show stable movement representation on software. Finally, the outcomes ranges show an alternative tool to evaluate patients with a forearm injury.

Subjective feelings, EMG, Data Set

Resumen

Actualmente, retroalimentaciones subjetivas son comúnmente empleadas para evaluar pacientes con lesión de antebrazo, sin ofrecer datos en tiempo real, provocando resultados de recuperación no satisfactorios. Las innovaciones tecnológicas en rehabilitación asistida han evolucionado los sistemas de monitoreo en tiempo real. El artículo, presenta un asistente interactivo para evaluar la relación entre los patrones cinemáticos y las señales electromiografícas (EMG) presentes en movimientos de rehabilitación del antebrazo. Los sensores Leap Motion (LM) y Shimmer3 EMG leen el comportamiento del movimiento del antebrazo para seguir los objetivos programados en el software interactivo, los cuales son establecidos por el terapeuta para determinar el progreso de la recuperación. La integración de software y hardware, muestra un conjunto de datos basado en variables de interacción tales como: velocidad y posición del antebrazo, tasa de rendimiento y señales EMG. Los resultados obtenidos indican que el sistema puede funcionar eficazmente dentro de un rango de movimiento de 9 a 88 grados alrededor de los ejes de rotación, las velocidades por debajo de 190 mm/s ofrecen una representación estable en el software de interacción. Finalmente, los rangos de operación permiten al asistente interactivo ser una herramienta alternativa en la evaluación de pacientes con lesión del antebrazo.

Asistente Interactivo, EMG, Patrones cinemáticos

* Correspondence to Author (e-mail: fernando_jimenez@utcj.edu.mx)

† Researcher contributing as first author.

1 Introduction

Recent scientific evidence suggests to physicians and therapists in physical rehabilitation should be aware of the low rates of confidence in the subjective feedback of patients during the assessment of recovery or the assignment of high-impact rehabilitation routines (Van der Scheer, 2018). Modern technological development in physical patient rehabilitation assistants offers an objective data frame in injury evaluations related to arm, knee, hip, among others (Yandell, 2017), (Gupta, 2020), (Modi, 2020). Rehabilitation assistance systems are typically based on data capture devices, motion aids, and interactive software to evaluate patient therapy progress (Noveletto, 2018), (Van der Kuil, 2018). Data capture devices assist the quantification process of the movement routines evaluation (Yu, 2019). Variables of speed, acceleration, position, and strength are using as auxiliaries making decisions about the patient recovery process in exercise routines proposed by the professionals. Besides, some application systems use interactive guide software to manage the routine showing tangible benefits in rehabilitation process results (Alimanova, 2017).

Patients with forearm injury related to accidents such as stroke, fracture, or perforated wound (Se-Hun, 2019) require movement exercises as rehabilitation treatment assisted by a robotic person or rehabilitation device (Akdoğan, 2018). Kinematics variables such as velocity, position, acceleration, or even force quantify the performance related to radial deviation, flexion, and extension forearm exercises. The rehabilitation process usually takes a long period of time, especially when the professional therapists evaluate with clinical pain perception. From this point of view, the kinematics data set could be an auxiliary to improve the recovery process.

EMG signals are used to measure the electrical activity of muscles. Dividing muscles into sections is the most common way to extract features of the forearm electrical activity in flexion or extension movements. Moreover, the section division is useful to detect open-close movements of the hand (Jarque-Bou, 2019). Electrical activity in muscles shows a substantial difference in types of forearm movements.

Rehabilitation professionals use EMG signals to set perspective targets related to EMG response in exercise routines (Hedt, 2020).

In this paper, an interactive assistant tool is proposed as an evaluation alternative in forearm rehabilitation. The system links kinematics data to an interactive software developed in MATLAB, and EMG data is captured in parallel to describe the types of forearm movements. The main aim is to support evaluations reports of the recovery process providing quantify data from forearm performance in physical rehabilitation programs. Finally, an interactive game software complements the system with entertainment targets related to exercise routines programmed by therapists.

The rest of this paper is organized as follows. Section 2 presents related research. In Section 3, a description of the novel assistant tool is presented. Test results are presented in Section 4. Finally, Section 5 concludes the paper.

2. Related work

The literature evidence on devices and interfaces for motion recognition shows a trend in medical applications related to physical rehabilitation, elderly care, and physical conditioning of people. (Ignasiak ,2017), (Henriksen, 2018).

An interactive interface is typically used as a guide for developing movement routines with a medical intention of recovery. In addition, the development of interactive games prevents patients from getting bored or bothered by exercise routines. For example, Guneysu *et al.* (2018) presents an interactive rehabilitation process design based on the Celullo game with a set of tangible robots. The system guides the patient movement routine in a fun way, and the patient performs the routines at home. The design of the rehabilitation process is based on linking movements of the robot with forearm rehabilitation routine in the plane of the game. The results obtained in the ANOVA study show improvements in the performance of the arm movement in the exercise routine

The implementation of interactive games in maintenance therapy has had a boom in the treatment of Parkinson's disease.

Article

Fernández *et al.* (2019) presents a high level of satisfaction and compliance study based on integrating a signal acquisition device and non-invasive interactive games among patients with medium and moderate levels of the disease. The movement tests on the most affected side of the patient show a significant increase in skill coordination. However, more studies should be developed to verify signal acquisition device effectiveness.

Rotation joints detection is one of the main challenges to classify the movements of the forearm. Samad *et al.* (2017) presents a work based on a low-cost depth sensing device to find the rotation joint without markers through the angle measure of the elbow. The system classifies flexion and extension forearm movements by computing position vectors of the elbow. The results show the classified movements of five people according to the angle of rotation captured by the device.

Typically, EMG signals are the way to detect the starting impulse, which is defined as the electrical magnitude of the muscle when a force is applied. Pinzon *et al.* (2020) proposes a new hand movement recognition system, specially designed for signal processing, based on an EMG band capture device and filters processing as the mean square root and the Butterworth. The system is divided into two phases, the recognition of hand movements and the algorithm used to recognize muscle activity. Finally, the results show a satisfactory estimation of the muscular activity of four users without muscular injury.

Worldwide physical rehabilitation systems have evolved the way of evaluating recovery processes from physical injuries. Table 1 lists some of the works that have been performed on quantification movements systems. Each research project attempts to solve a specific problem in any part of the human body and uses different technologies, such as robotic systems, sensors, and interactive interfaces.

| Autor/year	Application	Signals	Interface
Jie *et al.* (2017)	Interactive upper limb rehabilitation device in elderly patients who have suffered a stroke	Force, Rotation angle	Interactive simulation of daily life activity.
Dehem *et al.* (2017)	Robotic assist game for motor and cognitive rehabilitation after a stroke	Force, Position	Position targets with distracting elements
Lyu *et al.* (2019)	Development of an exoskeleton for the knee, in an interactive game context	EMG	Control bird flight, to avoid obstacles, the stability of the flight is through EMG signals
Ghassemi *et al.* (2019)	Development of an interactive game control through EMG signals, using the muscular activity of the hand.	EMG	Interactive scenarios for different exercises, such as revealing images, or solving a maze.
Daoud *et al.* (2020)	Rehabilitation study of patients with cerebral palsy, through a depth sensing device, which identifies the movements of the right arm.	Position	It is based on 3 interactive games, which guide the patient to follow the movement routine.

Table 1 Related work of rehabilitation assistant developing

Assistants in physical rehabilitation systems face several developing obstacles. For example, the elderly could be unfamiliar with technological systems. Developing simple alternatives could be an auxiliary to improve the way an elder interacts with rehabilitation assistants.

The literature review exposes some areas of opportunity that have not been explored at all, such as sensor fusion in interactive interfaces as a quantitative evaluation tool of the patients on the recovery process from a forearm injury. The present work shows an alternative sensor fusion tool of two capture sources (kinematic and EMG) that are contained through an interaction guide interface to evaluate the forearm movements in the three freedom degrees defined by Palma et al. (2021).

3. Design proposal

The interactive assistant tool is based on a multi-level operation design, using non-invasive real-time signal acquisition methods. The model is divided into four application levels: 1. Capture Device (Configuration and Calibration); 2. Targets programming in the interactive interface; 3. Real-time signal processing during routine; 4. Results of the work. Figure 1 shows the general scheme of the tool.
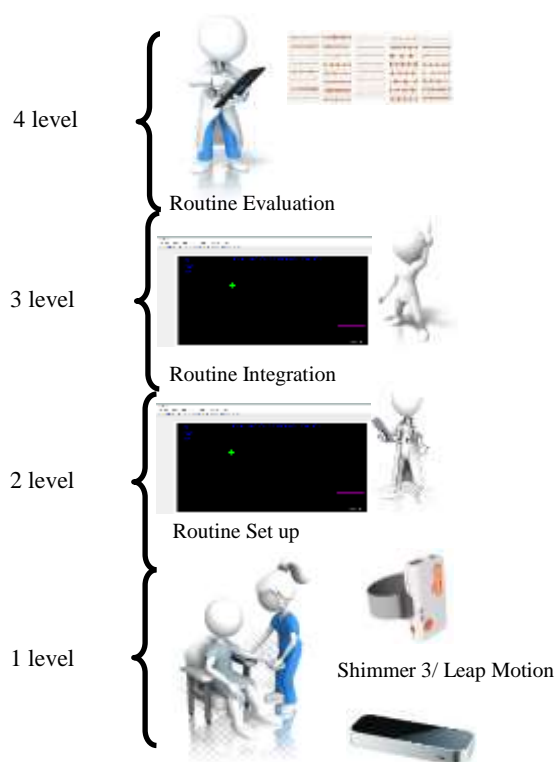

Figure 10 General schematic of the interactive assistant tool.

Each device is configured according to the individual specifications of the equipment, then the movement targets are programmed for the evaluation, which can be flexion, extension, supination, among others. The interface guides the patient in a fun interaction, where the kinematic variables and EMG are captured and processed.

Finally, the dataset of movements, positions, speeds, the electrical intensity of the muscle, and targets performance rate are presented as a result.

3.1 Signal Acquisition

The configuration and calibration of the acquisition devices are crucial to get objective evaluation results. The kinematic signals are obtained from Microsoft's Leap Motion (LM) device. The SDK package is used for communication and calibration with the interactive interface in the MATLAB programming environment. The anatomic structure connection of the hand and forearm allows obtaining the variables of position and speed of the forearm movements through the representation of the hand in real-time captured by the LM device. Figure 2 shows the relationship to capture kinematic signals.

(a)   (b)

(c)   (d)
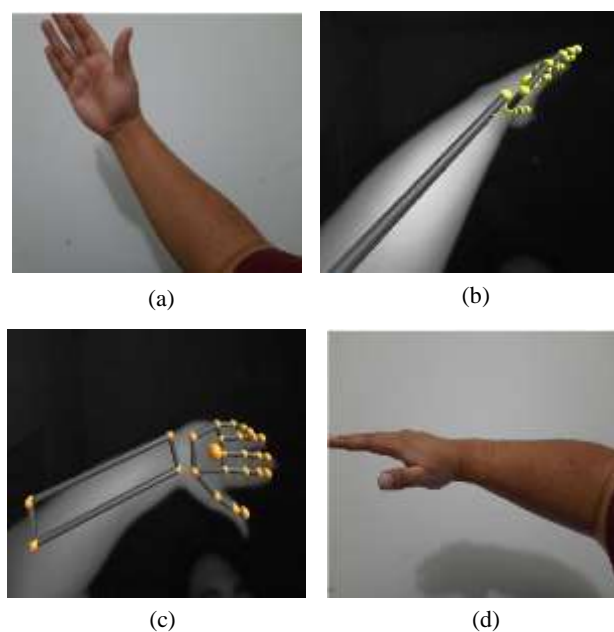
Figure 11 a) Extension; b) LM extension; c) LM flexion; d) Flexion

Figure 2 shows the orientation of the forearm through the LM device using the hand position. The patient should keep the hand orientation in the same direction as the forearm, it is important to avoid dropping or lifting the hand above the plane of the forearm. The ideal position to keep recognition stability is 250 mm above the sensor. (Vysocký, 2020)**.** The acquisition of EMG signals was developed through a Shimmer 3 EMG device, which is a non-invasive device that wirelessly sends the electrical activity of the muscle through activation channels, even in muscular injured tissue.

Typically, the range of EMG signal range operating frequencies is from 20 Hz to 500 Hz and the oscillation in voltage amplitudes is from 50 µV to 5 mV (González-Mendoza,2018)**.** Vidar *et al.* (2021) recommends the preparation of the muscle areas where the capture electrodes will be positioned as a first step. Routine movements data are processed using a band-pass filter. The filtered data is analyzed employing statistical tools for subsequent presentation in the results of the interaction. Table 2 shows the position of the electrodes related to muscle and movement.

Muscle	Movement Types	Electrode position
Arm biceps	Internal Rotation	
Arm biceps	Flexion - Extension	
Brachioradial	Supination	
Extender extensor of carpals of the radius	Wrist flexion/extension	

**Table 2** Relationship of the electrode position for EMG signal capture

The red dots represent the electrodes, which capture the electrical pulses from the muscle, while the blue dot represents the reference. It is crucial to clean impurities from the skin to reduce the impedance effect of the human body. The data will be received wirelessly through Wi-Fi for further analysis.

3.2 Software Interface

The proposed interface development uses a virtual entertainment environment to increase patient interest.

The patient should follow a virtual ball movement to hit it with a bar in a specific position and area.

The movement bar helps the patient performing the correct forearm exercises to score points. The patient gets rewards points by hitting the virtual ball in the specific orientation proposed by the therapist. The interface was developed in the MATLAB environment. The position and orientation of the hitting bar are associated with the LM device information. Figure 3 shows an example of using the bar orientation to perform the flexion-extension movement during a game therapy session.

(a)

(b)

(c)
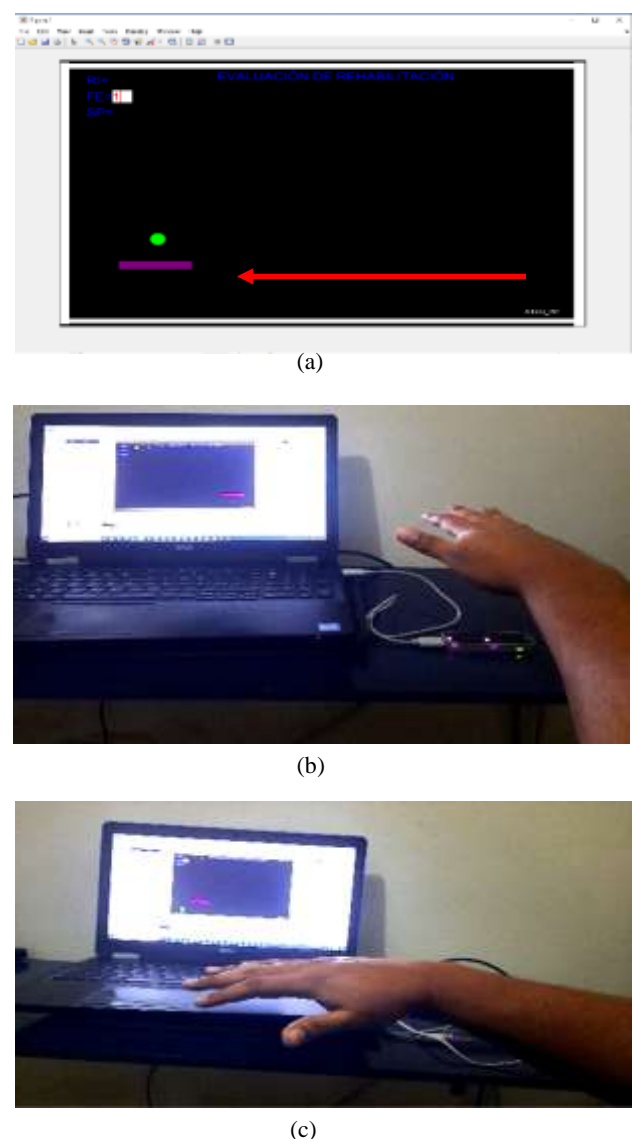
Figure 12 Interaction interface screen with flexion motion. a: Interface; b: Initial position; c: End position.

The patient hits the virtual ball with the flexion movement from the initial point to the final point. A new target appears when the patient hits the ball restarting the operation. Then the patient should extend the forearm to the initial position to begin a correct movement.

The exercise ends when the patient reaches the number of flexions and extensions proposed by the therapist or fails two times hitting the ball.

A failure is determined when the ball exceeds the horizontal or vertical plane of the bar, depending on the exercise. The number of failures was set at two per exercise.

In the beginning, the rehabilitation professional must select the forearm to be exercised (right or left), the types of movements (internal rotation, flexion, extension, supination), and the number of times movements to repeat during the exercise. Besides, the registry saves the personal data of the patient. The software uses the data entered by the professional to create the different instances of the virtual ball and the orientation of the hit bar. Hit bar appears at each turn of the interface, depending on the type of exercise. The setting section is an interface that was created using the MATLAB package (GUI) tool to support the professionals to set the routine. Figure 4. Shows the setting screen of the interface.
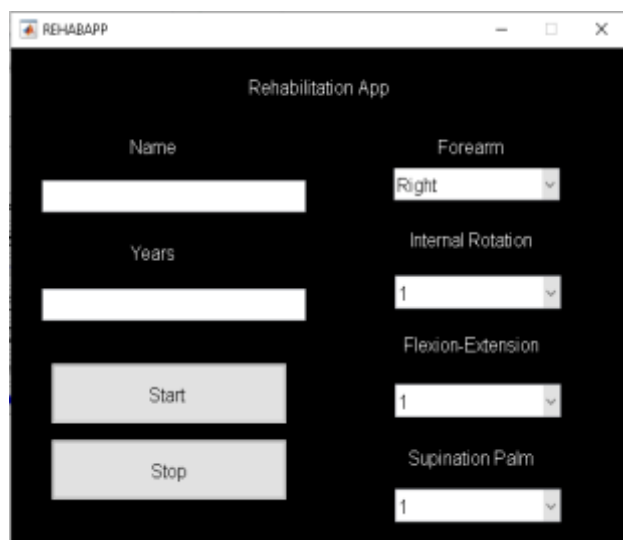

Figure 13 Setting window interface

The motion programming selection determines the direction of the bar. For example, an internal rotation computes the rotation matrix to represent it in the screen in the correct position then the user could hit the ball to get the right points. Equation 1 shows the matrix used to determine the direction of the bar with lengths in pixels.

$$\begin{aligned} p_x \\ p_y \end{aligned} = \begin{pmatrix} \cos\theta & -\sin\theta \\ \sin\theta & \cos\theta \end{pmatrix} \begin{pmatrix} l_{px} \\ l_{py} \end{pmatrix} \qquad (1)$$

Where p_x, p_y, are the final vector position in pixels, θ, is the internal rotation angle that the patient should emulate, and l_{px}, l_{py} are the fixed lengths of the hit bar in pixels.

Figure 5 shows the display of the associated internal rotational motion for the rebound of the virtual ball. Finally, the game view changes to vertical to obtain points at different degrees in the internal rotation exercise.
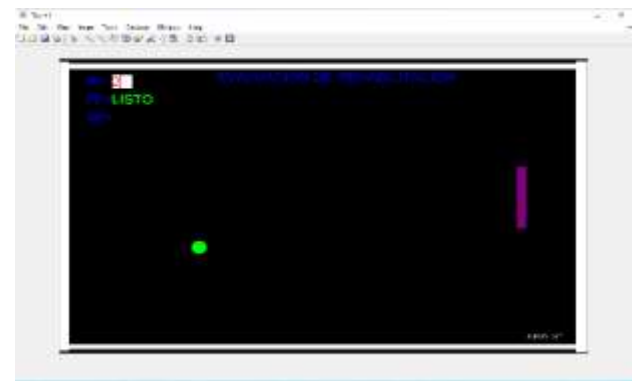

(a)

(b)

Figure 14 Internal rotation movement. a: Interface; b: Direction of the forearm

Other essential exercises are supination and palm orientation, in which the horizontal bar rotates 360 degrees and the ball is on the opposite side from the current palm location. Besides, time is monitored while the patient moves the forearm to the correct direction under the virtual ball as sufficient evidence of supination. Figure 6 shows an extract of the horizontally moving point algorithm.
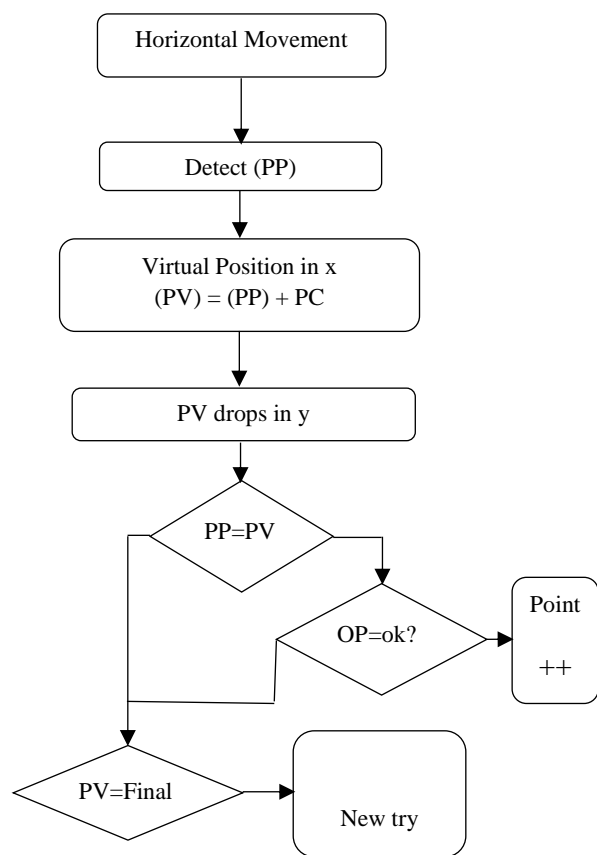
Figure 15 Horizontal movement. Palm position (PP), Virtual Ball Position (PV), Opposite Constant position (PC), Palm direction (OP)

During the exercise, the patient faces several shifts, where the virtual ball will appear at different points of the virtual environment, with distinct kinematic movement challenges. As an alternative, ConsensysPro Software captures the EMG signals results of the shift interaction present in each movement. Finally, MATLAB statistical tools process the EMG signals and characterize the movements in voltage amplitude (mv). Figure 7 shows the interaction of the Shimmer3 EMG sensor with the gaming interface.

Figure 16 Shimmer3 EMG sensor interface

3.3 Routine Evaluation

When the user completes the interactive exercises, the interface presents the data set in kinematic variables, targets achieved, and EMG signal ranges. Table 3 shows the output configuration array associated with patient performance in the kinematic model.

Movement velocity	Rotation angle x	Rotation angle y
Mean	Max	Max
Max	Min	Min

Table 3 Kinematics Dataset Structure

For the evaluation of the targets, the interface compares the planned targets with the satisfactory ones. A satisfactory target is when the patient hits the virtual ball with the right orientation and position. Table 4 shows the output configuration array associated with the performance of achieved targets.

M. Internal Rotation	M. Flexion and extension	M. Supination and palm
M. Planned	M. Planned	M. Planned
M. Achieved	M. Achieved	M. Achieved
% Satisfactory	% Satisfactory	% Satisfactory

Table 4 Performance Dataset Structure

For EMG signals associated with interactive exercises, the system uses the maximum and minimum voltage amplitude to classify the results of the movements. For example, when the user performs three flexion movements, the system computes maximum and minimum mean values in mv. Table 5 shows the output configuration array associated with the EMG performance of achieved targets.

Movement	Max	Min
Internal Rotation	Mean Max	Mean Min
Flexion and extension	Mean Max	Mean Min
Supination and palm	Mean Max	Mean Min

Table 5 EMG Dataset Structure

The results screen displays the final score performance helping the therapist with a quantitative exercise routine evaluation. Figure 8 shows the session results screen.
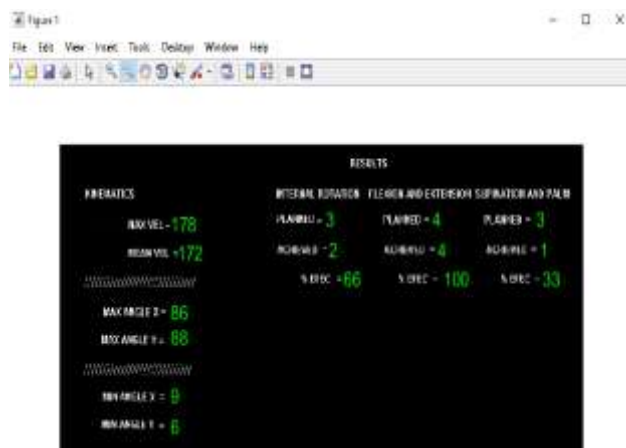
Figure 17 Final Results Screen

4. Results

Several experiments were developed to find the operating parameters of the assistant tool. At the first level, it is important to determine the operating range of the LM device interacting with the interface. Two tests were designed to evaluate the repeatability and reproducibility indices of the representation of the hit bar with respect to the patient hand position. Horizontal and vertical marks were used to define the limits of the flexion, extension, and internal rotation movements.

Twenty-seven horizontal and vertical movements were performed, divided into three healthy patients, and three different position marks at 0°, 45°, 90°. The dataset is the achieved positions from the patients. The device repeatability results are shown in Figure 9, grouped by test type.
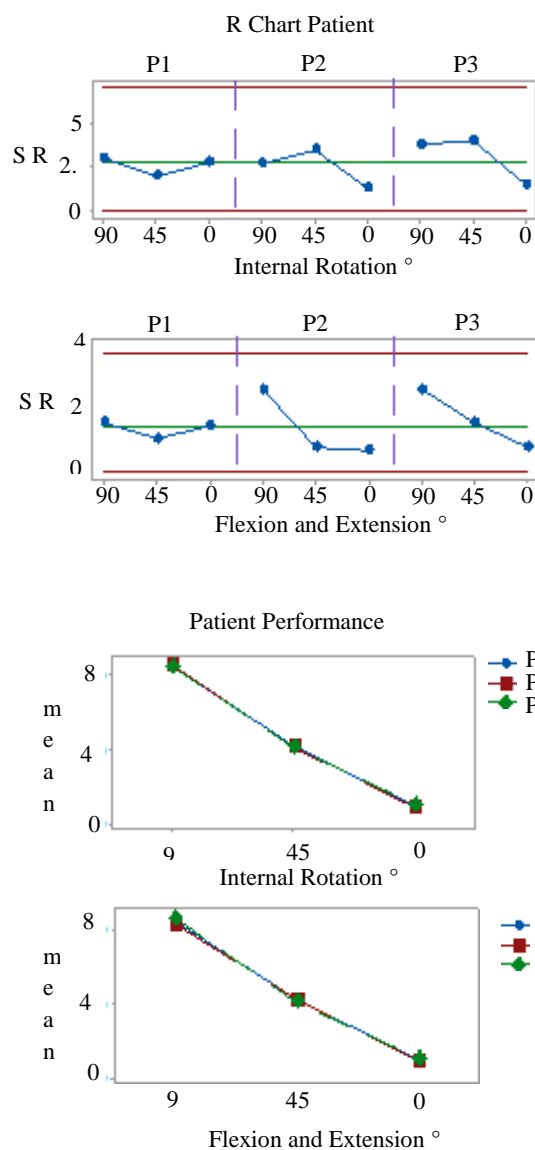

Figure 18 Repeatability studies by movement type

In the results, the repeatability of the flexion-extension and internal rotation movements is about 3% and 4%, respectively, which gives reliability that the device and interface are capable of providing correct data on the location of the forearm in response to the movement of the patient.

The maximum limit operating speed is 190 mm/s. The repeatability reduces the performances with values above the max limit. The minimum flexion-extension and internal rotation range that the device and interface detect are 9 to 88 degrees maximum. Five healthy patient sessions were used to compute the operating ranges at a minimum distance of $Dx\_min = 100$ mm, and $Dy\_min = 180$ mm above the LM, for the start of the session. Figure 10. Shows the ideal initial position for interacting with the interface.
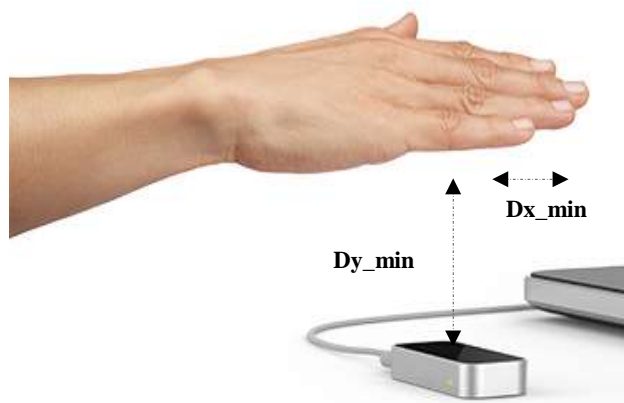
Figure 19 Position (x,y), start position of the session

Testing of the Shimmer 3 EMG device was based on establishing the maximum and minimum ranges of voltage amplitude for the different types of movements related to the performance of the patient in the routine session. Twenty samples of five distinct movements were taken to test the EMG signals. Figure 11 shows the minimum and maximum results of five types of movements presented in the interface.
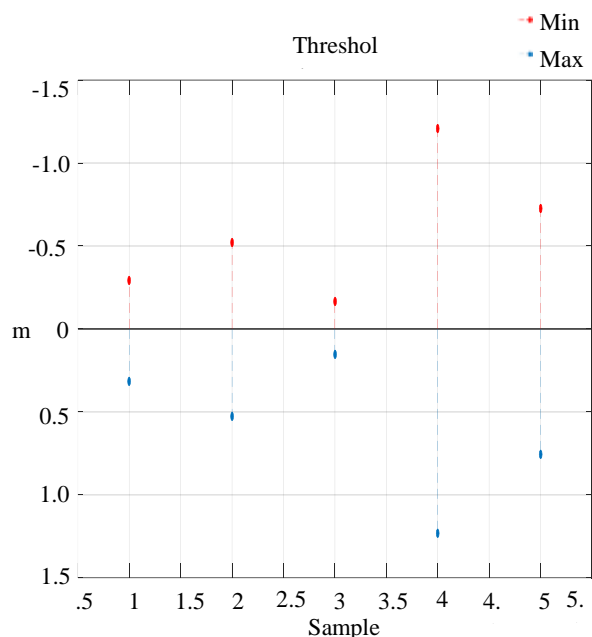
Figure 20 Voltage amplitude. Maximums and minimums per movement

There is a difference in the threshold voltage magnitude between patient movements in the results. Each movement is classified by the EMG signals values in the routine. In full session results, five test subjects developed a session of interaction with the interface, presenting quantitative results in velocities, positions, and EMG signals.

Besides, achievement target evaluation is presented. Table 6 shows some of the results of the full sessions.

Patient	Max Vel	% IR	% FE	% REMG
1	172 mm/s	92	100	90
2	178 mm/s	95	100	92
3	189 mm/s	98	100	95
4	170 mm/s	95	90	92
5	180 mm/s	100	100	95

Table 6 Full session results: IR Internal Rotation, FE Flexion Extension, REMG Relation with EMG signals
.

5. Conclusions

In this paper, an interactive assistant tool was presented as an evaluation alternative to capture quantitative variables of patients with a forearm injury. Sometimes rehabilitation routines could be boring or bothering for the patient, so the work intends to offer an entertaining alternative to the patient when performing the rehabilitation routine or evaluation. In addition, a reliable data set is providing related to variables from forearm movements.

In conclusion, the improvements presented by the interactive tool to monitor the recovery process are:

– Clinical diagnosis support by quantitative evaluation reports in the forearm recovery process.
– The patient develops exercises therapy through the programming routines proposed by professionals in an entertainment environment.
– Sensor fusion of multiple variables (kinematics and EMG) defines the forearm movements to monitor the recovery progress.

Finally, the project begins as an academic-technological development in the area of assisted physical rehabilitation. However, the project evolved until it produced an application for medical services. The operation ranges allow the interactive tool to be an alternative application in the evaluation processes of forearm injuries. In future works, the development of a driver to include both signals in the same game interface is the target, as well as to deploy Artificial Intelligent models to define automatic exercise routines.

6. References

Akdoğan, E., Aktan, M. E., Koru, A. T., Arslan, M. S., Atlıhan, M., & Kuran, B. (2018). Hybrid impedance control of a robot manipulator for wrist and forearm rehabilitation: Performance analysis and clinical results. Mechatronics, 49, 77-91.

Alimanova, M., Borambayeva, S., Kozhamzharova, D., Kurmangaiyeva, N., Ospanova, D., Tyulepberdinova, G., ... & Kassenkhan, A. (2017, April). Gamification of hand rehabilitation process using virtual reality tools: Using leap motion for hand rehabilitation. In 2017 First IEEE International Conference on Robotic Computing (IRC) (pp. 336-339). IEEE.

Andersen, V., Pedersen, H., Steiro Fimland, M., Peter Shaw, M., Jorung Solstad, T. E., Stien, N. ... & Hole Saeterbakken, A. (2021). Efectos Agudos de las Bandas Elásticas como Resistencia o Asistencia sobre la EMG, la Cinética y la Cinemática durante el Peso Muerto en Hombres Entrenados en Fuerza-Ciencias del Ejercicio. Revista de Educación Física, 1(1).

Daoud, M. I., Alhusseini, A., Ali, M. Z., & Alazrai, R. (2020). A Game-Based Rehabilitation System for Upper-Limb Cerebral Palsy: A Feasibility Study. Sensors, 20(8), 2416.

Fernández-González, P., Carratalá-Tejada, M., Monge-Pereira, E., Collado-Vázquez, S., Baeza, P. S. H., Cuesta-Gómez, A., ... & Cano-de la Cuerda, R. (2019). Leap motion-controlled video game-based therapy for upper limb rehabilitation in patients with Parkinson's disease: a feasibility study. Journal of neuroengineering and rehabilitation, 16(1), 1-10.

Ghassemi, M., Triandafilou, K., Barry, A., Stoykov, M. E., Roth, E., Mussa-Ivaldi, F. A., .. & Ranganathan, R. (2019). Development of an EMG-controlled serious game for rehabilitation. IEEE Transactions on Neural Systems and Rehabilitation Engineering, 27(2), 283-292.

González-Mendoza, A., Pérez-SanPablo, A. I., López-Gutiérrez, R., & Quiñones-Urióstegui, I. (2018, September). Validation of an EMG sensor for Internet of Things and Robotics. In 2018 15th International Conference on Electrical Engineering, Computing Science and Automatic Control (CCE) (pp. 1-5). IEEE.

Guneysu Ozgur, A., Wessel, M. J., Johal, W., Sharma, K., Özgür, A., Vuadens, P., ... & Dillenbourg, P. (2018, February). Iterative design of an upper limb rehabilitation game with tangible robots. In Proceedings of the 2018 ACM/IEEE International Conference on Human-Robot Interaction (pp. 241-250).

Gupta, A., Singh, A., Verma, V., Mondal, A. K., & Gupta, M. K. (2020). Developments and clinical evaluations of robotic exoskeleton technology for human upper-limb rehabilitation. Advanced Robotics, 34(15), 1023-1040.

Hedt, C., Lambert, B. S., Daum, J., Pearson, J. M., & McCulloch, P. C. (2020). Forearm position matters during eccentric shoulder exercises: an EMG recruitment study with implications for rehabilitation. International Journal of Sports Physical Therapy, 15(6), 1110.

Heins, S., Dehem, S., Montedoro, V., Dehez, B., Edwards, M., Stoquart, G., ... & Lejeune, T. (2017, April). Robotic-assisted serious game for motor and cognitive post-stroke rehabilitation. In 2017 IEEE 5th International Conference on Serious Games and Applications for Health (SeGAH) (pp. 1-8). IEEE.

Henriksen, A., Mikalsen, M. H., Woldaregay, A. Z., Muzny, M., Hartvigsen, G., Hopstock, L. A., & Grimsgaard, S. (2018). Using fitness trackers and smartwatches to measure physical activity in research: analysis of consumer wrist-worn wearables. Journal of medical Internet research, 20(3), e110.

Ignasiak, D., Rüeger, A., & Ferguson, S. J. (2017). Multi-segmental thoracic spine kinematics measured dynamically in the young and elderly during flexion. Human movement science, 54, 230-239.

Jarque-Bou, N. J., Vergara, M., Sancho-Bru, J. L., Gracia-Ibáñez, V., & Roda-Sales, A. (2019). A calibrated database of kinematics and EMG of the forearm and hand during activities of daily living. Scientific data, 6(1), 1-11.

Jie, S., Haoyong, Y., Chaw, T. L., Chiang, C. C., & Vijayavenkataraman, S. (2017). An interactive upper limb rehab device for elderly stroke patients. Procedia CIRP, 60, 488-493.

Lyu, M., Chen, W. H., Ding, X., Wang, J., Pei, Z., & Zhang, B. (2019). Development of an EMG-controlled knee exoskeleton to assist home rehabilitation in a game context. Frontiers in neurorobotics, 13, 67.

Modi, N., & Singh, J. (2020). A survey of research trends in assistive technologies using information modelling techniques. Disability and Rehabilitation: Assistive Technology, 1-19.

Noveletto, F., Soares, A. V., Mello, B. A., Sevegnani, C. N., Eichinger, F. L. F., Hounsell, M. D. S., & Bertemes-Filho, P. (2018). Biomedical serious game system for balance rehabilitation of hemiparetic stroke patients. IEEE Transactions on Neural Systems and Rehabilitation Engineering, 26(11), 2179-2188.

Palma, F. H., Cifre, M. J., Mancilla, I. C., Flores-León, A., & Guzmán-Venegas, R. (2021). Activación de los músculos escapulohumerales superficiales en tres planos distintos de elevación del hombro. Journal of Movement & Health, 18(2).

Park, S. H., Yi, J., Kim, D., Lee, Y., Koo, H. S., & Park, Y. L. (2019, April). A lightweight, soft wearable sleeve for rehabilitation of forearm pronation and supination. In 2019 2nd IEEE International Conference on Soft Robotics (RoboSoft) (pp. 636-641). IEEE.

Pinzón-Arenas, J. O., Jiménez-Moreno, R., & Rubiano, A. (2020). Percentage estimation of muscular activity of the forearm by means of EMG signals based on the gesture recognized using CNN. Sensing and Bio-Sensing Research, 29, 100353.

Samad, R., Bakar, M. Z. A., Pebrianti, D., Mustafa, M., & Abdullah, N. R. H. (2017). Elbow Flexion and Extension Rehabilitation Exercise System Using Marker-less Kinect-based Method. International Journal of Electrical & Computer Engineering (2088-8708), 7(3).

Van der Kuil, M. N., Visser-Meily, J., Evers, A. W., & Van der Ham, I. J. (2018). A usability study of a serious game in cognitive rehabilitation: a compensatory navigation training in acquired brain injury patients. Frontiers in psychology, 9, 846.

Van der Scheer, J. W., Hutchinson, M. J., Paulson, T., Ginis, K. A. M., & Goosey-Tolfrey, V. L. (2018). Reliability and validity of subjective measures of aerobic intensity in adults with spinal cord injury: a systematic review. PM&R, 10(2), 194-207.

Vysocký, A., Grushko, S., Oščádal, P., Kot, T., Babjak, J., Jánoš, R., ... & Bobovský, Z. (2020). Analysis of Precision and Stability of Hand Tracking with Leap Motion Sensor. Sensors, 20(15), 4088.

Yandell, M. B., Quinlivan, B. T., Popov, D., Walsh, C., & Zelik, K. E. (2017). Physical interface dynamics alter how robotic exosuits augment human movement: implications for optimizing wearable assistive devices. Journal of neuroengineering and rehabilitation, 14(1), 1-11.

Yu, X., & Xiong, S. (2019). A dynamic time warping based algorithm to evaluate kinect-enabled home-based physical rehabilitation exercises for older people. Sensors, 19(13), 2882.

Title in Times New Roman and Bold No. 14 in English and Spanish]

Surname (IN UPPERCASE), Name 1st Author†*, Surname (IN UPPERCASE), Name 1st Coauthor, Surname (IN UPPERCASE), Name 2nd Coauthor and Surname (IN UPPERCASE), Name 3rd Coauthor

Institutional Affiliation of Author including Dependency (No.10 Times New Roman and Italic)

International Identification of Science - Technology and Innovation

ID 1st Author: (ORC ID - Researcher ID Thomson, arXiv Author ID - PubMed Author ID - Open ID) and CVU 1st author: (Scholar-PNPC or SNI-CONACYT) (No.10 Times New Roman)

ID 1st Coauthor: (ORC ID - Researcher ID Thomson, arXiv Author ID - PubMed Author ID - Open ID) and CVU 1st coauthor: (Scholar or SNI) (No.10 Times New Roman)

ID 2nd Coauthor: (ORC ID - Researcher ID Thomson, arXiv Author ID - PubMed Author ID - Open ID) and CVU 2nd coauthor: (Scholar or SNI) (No.10 Times New Roman)

ID 3rd Coauthor: (ORC ID - Researcher ID Thomson, arXiv Author ID - PubMed Author ID - Open ID) and CVU 3rd coauthor: (Scholar or SNI) (No.10 Times New Roman)

(Report Submission Date: Month, Day, and Year); Accepted (Insert date of Acceptance: Use Only ECORFAN)

Abstract (In English, 150-200 words)

Objectives
Methodology
Contribution

Keywords (In English)

Indicate 3 keywords in Times New Roman and Bold No. 10

Abstract (In Spanish, 150-200 words)

Objectives
Methodology
Contribution

Keywords (In Spanish)

Indicate 3 keywords in Times New Roman and Bold No. 10

* Correspondence to Author (example@example.org)
† Researcher contributing as first author.

Instructions for Scientific, Technological and Innovation Publication

Introduction

Text in Times New Roman No.12, single space.

General explanation of the subject and explain why it is important.

What is your added value with respect to other techniques?

Clearly focus each of its features

Clearly explain the problem to be solved and the central hypothesis.

Explanation of sections Article.

## Development of headings and subheadings of the article with subsequent numbers

[Title No.12 in Times New Roman, single spaced and bold]

Products in development No.12 Times New Roman, single spaced.

## Including graphs, figures and tables-Editable

In the article content any graphic, table and figure should be editable formats that can change size, type and number of letter, for the purposes of edition, these must be high quality, not pixelated and should be noticeable even reducing image scale.

[Indicating the title at the bottom with No.10 and Times New Roman Bold]
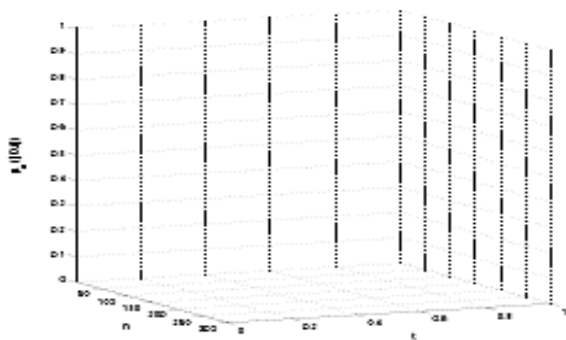
Graphic 1 Title and *Source (in italics)*

Should not be images-everything must be editable.
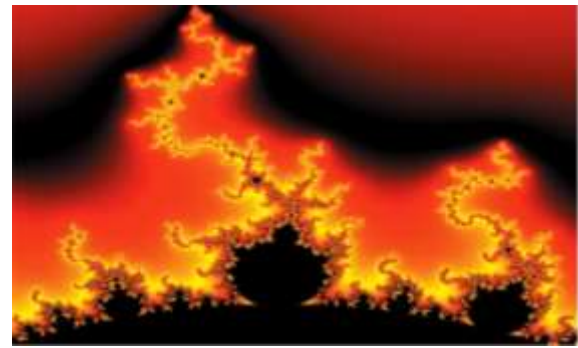
Figure 1 Title and *Source (in italics)*

Should not be images-everything must be editable.

Table 1 Title and *Source (in italics)*

Should not be images-everything must be editable.

Each article shall present separately in **3 folders**: a) Figures, b) Charts and c) Tables in .JPG format, indicating the number and sequential Bold Title.

For the use of equations, noted as follows:

$$Y_{ij} = \alpha + \sum_{h=1}^{r} \beta_h X_{hij} + u_j + e_{ij} \qquad (1)$$

Must be editable and number aligned on the right side.

Methodology

Develop give the meaning of the variables in linear writing and important is the comparison of the used criteria.

Results

The results shall be by section of the article.

Annexes

Tables and adequate sources

Thanks

Indicate if they were financed by any institution, University or company.

Surname (IN UPPERCASE), Name 1st Author, Surname (IN UPPERCASE), Name 1st Coauthor, Surname (IN UPPERCASE), Name 2nd Coauthor and Surname (IN UPPERCASE), Name 3rd Coauthor. Paper TitleJournal of Technological Engineering. Year [Times New Roman No. 8]

Conclusions

Explain clearly the results and possibilities of improvement.

References

Use APA system. Should not be numbered, nor with bullets, however if necessary numbering will be because reference or mention is made somewhere in the Article.

Use Roman Alphabet, all references you have used must be in the Roman Alphabet, even if you have quoted an Article, book in any of the official languages of the United Nations (English, French, German, Chinese, Russian, Portuguese, Italian, Spanish, Arabic), you must write the reference in Roman script and not in any of the official languages.

Technical Specifications

Each article must submit your dates into a Word document (.docx):

Journal Name
Article title
Abstract
Keywords
Article sections, for example:

1. Introduction
2. Description of the method
3. Analysis from the regression demand curve
4. Results
5. Thanks
6. Conclusions
7. References

Author Name (s)
Email Correspondence to Author
References

Intellectual Property Requirements for editing:

-Authentic Signature in Color of <u>Originality Format</u> Author and Coauthors

-Authentic Signature in Color of the <u>Acceptance Format</u> of Author and Coauthors

Reservation to Editorial Policy

Journal of Technological Engineering reserves the right to make editorial changes required to adapt the Articles to the Editorial Policy of the Research Journal. Once the Article is accepted in its final version, the Research Journal will send the author the proofs for review. ECORFAN® will only accept the correction of errata and errors or omissions arising from the editing process of the Research Journal, reserving in full the copyrights and content dissemination. No deletions, substitutions or additions that alter the formation of the Article will be accepted.

Code of Ethics - Good Practices and Declaration of Solution to Editorial Conflicts

Declaration of Originality and unpublished character of the Article, of Authors, on the obtaining of data and interpretation of results, Acknowledgments, Conflict of interests, Assignment of rights and Distribution

The ECORFAN-Mexico, S.C Management claims to Authors of Articles that its content must be original, unpublished and of Scientific, Technological and Innovation content to be submitted for evaluation.

The Authors signing the Article must be the same that have contributed to its conception, realization and development, as well as obtaining the data, interpreting the results, drafting and reviewing it. The Corresponding Author of the proposed Article will request the form that follows.

Article title:

– The sending of an Article to Journal of Technological Engineering emanates the commitment of the author not to submit it simultaneously to the consideration of other series publications for it must complement the Format of Originality for its Article, unless it is rejected by the Arbitration Committee, it may be withdrawn.

– None of the data presented in this article has been plagiarized or invented. The original data are clearly distinguished from those already published. And it is known of the test in PLAGSCAN if a level of plagiarism is detected Positive will not proceed to arbitrate.

– References are cited on which the information contained in the Article is based, as well as theories and data from other previously published Articles.

– The authors sign the Format of Authorization for their Article to be disseminated by means that ECORFAN-Mexico, S.C. In its Holding Taiwan considers pertinent for disclosure and diffusion of its Article its Rights of Work.

– Consent has been obtained from those who have contributed unpublished data obtained through verbal or written communication, and such communication and Authorship are adequately identified.

– The Author and Co-Authors who sign this work have participated in its planning, design and execution, as well as in the interpretation of the results. They also critically reviewed the paper, approved its final version and agreed with its publication.

– No signature responsible for the work has been omitted and the criteria of Scientific Authorization are satisfied.

– The results of this Article have been interpreted objectively. Any results contrary to the point of view of those who sign are exposed and discussed in the Article.

Copyright and Access

The publication of this Article supposes the transfer of the copyright to ECORFAN-Mexico, SC in its Holding Taiwan for its Journal of Technological Engineering, which reserves the right to distribute on the Web the published version of the Article and the making available of the Article in This format supposes for its Authors the fulfilment of what is established in the Law of Science and Technology of the United Mexican States, regarding the obligation to allow access to the results of Scientific Research.

Article Title:

Name and Surnames of the Contact Author and the Coauthors	Signature
1.	
2.	
3.	
4.	

Principles of Ethics and Declaration of Solution to Editorial Conflicts

Editor Responsibilities

The Publisher undertakes to guarantee the confidentiality of the evaluation process, it may not disclose to the Arbitrators the identity of the Authors, nor may it reveal the identity of the Arbitrators at any time.

The Editor assumes the responsibility to properly inform the Author of the stage of the editorial process in which the text is sent, as well as the resolutions of Double-Blind Review.

The Editor should evaluate manuscripts and their intellectual content without distinction of race, gender, sexual orientation, religious beliefs, ethnicity, nationality, or the political philosophy of the Authors.

The Editor and his editing team of ECORFAN® Holdings will not disclose any information about Articles submitted to anyone other than the corresponding Author.

The Editor should make fair and impartial decisions and ensure a fair Double-Blind Review.

Responsibilities of the Editorial Board

The description of the peer review processes is made known by the Editorial Board in order that the Authors know what the evaluation criteria are and will always be willing to justify any controversy in the evaluation process. In case of Plagiarism Detection to the Article the Committee notifies the Authors for Violation to the Right of Scientific, Technological and Innovation Authorization.

Responsibilities of the Arbitration Committee

The Arbitrators undertake to notify about any unethical conduct by the Authors and to indicate all the information that may be reason to reject the publication of the Articles. In addition, they must undertake to keep confidential information related to the Articles they evaluate.

Any manuscript received for your arbitration must be treated as confidential, should not be displayed or discussed with other experts, except with the permission of the Editor.

The Arbitrators must be conducted objectively, any personal criticism of the Author is inappropriate.

The Arbitrators must express their points of view with clarity and with valid arguments that contribute to the Scientific, Technological and Innovation of the Author.

The Arbitrators should not evaluate manuscripts in which they have conflicts of interest and have been notified to the Editor before submitting the Article for Double-Blind Review.

Responsibilities of the Authors

Authors must guarantee that their articles are the product of their original work and that the data has been obtained ethically.

Authors must ensure that they have not been previously published or that they are not considered in another serial publication.

Authors must strictly follow the rules for the publication of Defined Articles by the Editorial Board.

The authors have requested that the text in all its forms be an unethical editorial behavior and is unacceptable, consequently, any manuscript that incurs in plagiarism is eliminated and not considered for publication.

Authors should cite publications that have been influential in the nature of the Article submitted to arbitration.

Information services

Indexation - Bases and Repositories

RESEARCH GATE (Germany)
GOOGLE SCHOLAR (Citation indices-Google)
MENDELEY (Bibliographic References Manager)
REDIB (Ibero-American Network of Innovation and Scientific Knowledge- CSIC)
HISPANA (Information and Bibliographic Orientation-Spain)

Publishing Services

Citation and Index Identification H
Management of Originality Format and Authorization
Testing Article with PLAGSCAN
Article Evaluation
Certificate of Double-Blind Review
Article Edition
Web layout
Indexing and Repository
ArticleTranslation
Article Publication
Certificate of Article
Service Billing

Editorial Policy and Management

69 Street. YongHe district, ZhongXin. Taipei-Taiwan. Phones: +52 1 55 6159 2296, +52 1 55 1260 0355, +52 1 55 6034 9181; Email: contact@ecorfan.org www.ecorfan.org

Journal of Technological Engineering

"Inductor Disc CFD Analysis for VAWT"
MARIN-TELLEZ, Gerardo Javier, LÓPEZ-GARZA, Víctor, MARIN-TELLEZ, Paulina and SANTIBAÑEZ-MALDONADO, Adrián
Universidad Michoacana de San Nicolás de Hidalgo

"CO_2 emissions of an asphalt pavement in kg of CO_2 per m^2"
LOPEZ-CHAVEZ, Oscar, MERCADO-IBARRA, Santa Magdalena, ACEVES-GUTIÉRREZ, Humberto and CAMPOY-SALGUERO, José Manuel
Instituto Tecnológico de Sonora

"Design and Construction of an ALD Reactor by Growth of Al_2O_3 Nanostructure Films"
MONTES-GUTIERREZ, Jorge, LOPEZ-GASTELUM, Ana, ROMO-GARCÍA, Frank and GARCIA-GUTIERREZ, Rafael
Universidad de Sonora

"Interactive assistant tool for the evaluation of kinematic patterns and EMG signals in patients with a forearm injury"
JIMÉNEZ-GONZÁLEZ, Fernando C. & TORRES-RAMÍREZ, Dulce *Esperanza*
Universidad Tecnológica de Ciudad Juárez